This is the accepted version of this paper. The version of record is available at https://doi.org/10.1016/j.tws.2021.108162

An experimental investigation on the effect of incorporating graphene nanoplatelets on thelow-velocity impact behavior of fiber metal laminates

Azadeh Fathi[a], Gholamhossein Liaghat[a,b,*], Hadi Sabouri[c]

[a]*Department of Mechanical Engineering, Faculty of Engineering, Tarbiat Modares University, Tehran, Iran*
[b]*School of Mechanical & Aerospace Engineering, Kingston University, London, UK*
[c]*Department of Mechanical Engineering, Faculty of Engineering, Kharazmi University, Tehran, Iran*

Abstract:

In this study, experimental investigations are implemented to evaluate the effect of incorporation of graphene nanoplatelets (GNPs) on the low-velocity impact behavior of composites and fiber metal laminates (FMLs). The hand layup technique is employed to fabricate composite specimens and FML panels with 2/1 configuration. Impact response and damage patterns of unmodified and modified specimens subjected to various impact energy levels are compared. The results reveal that the incorporating 0.2 wt% of GNPs strengthens the impact resistance of FMLs so that the modified panels possess higher bending stiffness,peak load, energy absorption and SEA compared to the unreinforced ones.Visual inspections and SEM images exhibit that the inclusion of GNPs enhances the adhesion between resin/fibers as well as composite plies, thereby reducing damage area and increasing penetration threshold of FMLs.In addition, reinforcing composite panels considerably improves the impact behavior in comparison with the unmodified composites.

Keywords: Low-velocity impact, Composite, Fiber metal laminate, Graphene nanoplatelets

[*]**Corresponding author:**
Department of Mechanical Engineering, TarbiatModares University, Tehran, Iran.
E-mail: Ghlia530@modares.ac.ir, G.Liaghat@kingston.ac.uk (G.Liaghat).

1 Introduction

Fiber metal laminates (FMLs) area family of hybrid materials that consist of thin metal layers and fiber reinforced composite laminates. By combining metal layers with composites (typically aluminum alloy sheets and glass/epoxy fiber laminates) the overall weight of resulting hybrid specimen in comparison with monolithic metals can be reduced, as well as properties such as the ability to delay and stop crack growth, damage tolerance and strength can be improved. These outstanding properties of FMLs, especially the high impact resistance, make them a suitable material for industrial applications, for instance, aircraft, aerospace and marine structures. Low-velocity impact, as one of the impact failure sources, can occur through damage from for example service trucks, cargo containers and dropped tools during maintenance operations of aircrafts[1–6].

In the 1990s, at the University of Delft, Vlot et al. conducted many tests, such as quasi-static test, low velocity and high velocity impact to investigate the dynamic behavior of FMLs. It was found that the FMLs had a much higher resistance than aluminum and composite layers against impact, also by comparing the FML types (ARALL, CARALL and GLARE), they concluded that GLARE had better impact properties and was able to absorb more energy[7–9]. After Vlot, during the last two decades, numerous researches have been performed to examine the impact behavior of the FMLs considering the effect of various parameters and factors, such as lay-up configuration[10–16], metal constituents[10,17–23], distribution of layers[24–26], thickness effect [19,27–29], impactor geometry [30–32], strain rate [33–36],repeated impact response[1,37–40] and damage area [26,41]. Additionally, Jakubczak et al. [42] evaluated the FML damage mechanisms at low energy impacts and reported that matrix fractures (at the fiber/matrix interface), fiber cracking, and delamination were the main modes of damage.The low-velocity impact damage is an important failure pattern in FML structures and complex damage modes make it more challenging to characterize the low-velocity impact behavior of FMLs [31].

Matrix reinforcement by incorporation of reinforcing phases into the matrix is a method of improving the mechanical properties and impact resistance of FMLs and many researchers have investigated the effect of

using nanofiller-modified matrix in manufacturing of FMLs in recent studies[3,43–51].Megahed et al.[52]investigated the mechanical characterization of FMLs by adding several types of nanofillers such as aluminum (Al), copper (Cu), titanium oxide (TiO_2), silica (SiO_2), aluminum oxide (Al_2O_3) and nano clay (NC).The experimental results indicated that since SiO2 nanomodification of the epoxy matrix led to an improved interfacial bonding between the nanophase epoxy matrix and fibers, and good bonding between outer metal layers and the nanocomposite laminate, a maximum improvement of 39%, 33.2% and 108.4% in tensile strength, modulus and toughness as compared to the unreinforced specimen were achieved. The effect of adding multi-walled carbon nanotubes (MWCNTs) on impact behavior of the FMLs is studied by several researchers [3,43,53,54]and it is stated that the incorporation of MWCNTs diversified the energy absorbing mechanisms in terms of nanotubes pull-out, debonding, and bridging effects, leading to improved impact performance of FMLs.

Graphene-based nanofillers were recently used to strengthen epoxy resin thus enhance the mechanical properties of nanocomposites[55–64]. For instance, an investigation conducted by Li et al. [49]showed that the Young's modulus, the tensile strength and the flexural performance of FMLs improved by inclusion of the graphene oxide (GO). This can be ascribed to the fact that the GO enhanced the interface strength between the aluminum and the epoxyand increased the load transmission capacity across the interface between fiber and epoxy in the FMLs.GNPs, as one of the most widely used nanoplatelets, have been able to enhance the properties and strength of composite[65–74]and FML specimens[5,75–79]. Furthermore, the significant improvements in strength, fracture toughness, and fatigue strength have been reported using graphene as fillers or reinforcements in nanocomposites[58].Domun et al.[70] studied the incorporation of GNPs at concentrations of 0.1, 0.25, 0.5, 0.75 and 1 wt% into epoxy resin and reported that maximum improvement in stiffness and fracture toughness was achieved in 0.25 wt%. This was attributed tothe preparation of homogenous dispersions of GNP in the nanocomposite, thereby increasing the performance significantly due to load transfer of the nanomaterials.Furthermore, Abbandanak et al.[77]stated thatflexural and impact properties of FMLs improved

by adding GNPs to epoxy. They explained the reason for this finding by the strong adhesion between the polymer and fibers within the composite interlayers, which led to considerable load transfer from matrix to the fiber.Moreover, a recent comparative study, investigated the quasi-static behavior of composite and FML panels modified by GNPs and reported that the inclusion of GNPsimproved the strength and fracture toughness of the composite and FML panels by delaying the failure modes[5].

According to the literature survey, despite the fact that the incorporation of nanofillers can improve the mechanical properties and enhance the impact and damage resistance of FMLs, the full potential of nano reinforcing of FMLs is not explored enough. In addition, although many studies have been examined on the modified epoxy resins and glass fiber composites, the researches about incorporating GNPs to FMLs are still in infancy.Moreover, to the best of the authors' knowledge, the effect of adding GNPs on the low-velocity impact response of FMLs has not been investigated yet. Consequently, in order to develop the application of FMLs, it is essential to conduct further investigation on the impact behavior of GNPs-reinforced FMLs.

Thus, the objective of this work is mainly to investigate the effect ofGNPs incorporation on the low-velocity impact behavior of composite and FML panels and also to identify and compare the damage modes of the unmodified and modified specimens. On the basis of the literature review, it can be expected that the presence of GNPs will enhance the bonding between the polymer and fiber, and the load transmission capacity from matrix to the fiber, thereby improving the impact and damage resistance of the specimens.To explore this, a series of the low-velocity impact tests including 33 J, 44 J and 82 J are conducted on the unreinforced and reinforced FML panels. In addition to the FMLs, composite specimens are studied to gain further insight into the effect of GNPs on the impact properties of the composite laminate of FMLs. The impact performance of specimens are assessed by comparingthe absorbed energy, the specific energy absorption (SEA), the peak load, and the maximum deflection of the unmodified and modified panels. Moreover, scanning electron microscopy (SEM), destructive cross–sectional technique, and non-destructive tests such as computed radiography (CR) and X-ray computed tomograhgy (X-CT) areemployed to elucidate the damage mechanisms. Furthermore, to

investigate the effect of strain rate on performance properties of FML panels, the results corresponding to impact tests are compared with those observed for identical panels subjected to quasi-static test reported in our previous work [5].

2 Experimental procedures

2.1 Materials

In current study, FMLs are manufactured with metallic layers and a composite laminate. 2024-T3 aluminum alloy sheets with a thickness of 0.5 mm per layer are selected as metallic layers in the FMLs, and the composite laminate is made of glass fiber, epoxy resin and graphene nanoplatelets.The properties of the materials investigated here are summarized in**Table 1**.

Table 1. Type and mechanical properties of materials.

Material	Type	Material properties
Aluminum	2024-T3	E=72 GPa, ρ=2700 kg/m^3, ν=0.3
E-Glass Fiber	Plain Woven	ρ_A=400 g/m^2, Nominal thickness=0.16 mm
Epoxy System	ML-506 (HA-11 hardener)	ρ=1.1 g/cm^3, Curing Temp. = Room Temp.(cold-cured), Gel Time = 24 min, Time to Max. Strength = 7 days
Graphene Nanoplatelets	XG Science Grade C	ρ=2.2 g/cm^3, SSA=750 m^2/g

2.2 Surface treatment of metal sheets

As bonding between polymeric composite laminate and metallic layers is a key issue for FMLs performance, thus an adequate surface treatment of the metallic layers is required [52]. Therefore, the surfaces of aluminum sheets are pretreated according to the ASTM D2651 [80] protocol at four steps. First, the aluminum sheets are washed with acetone. Second, they are degreased using an alkaline solution. Then, the surfaces are abraded by sandpaper [81] and abrasive particles and debris are rinsed from the surface by warm-to-hot water. Finally, the sheets are left at ambient conditions for about one hour before applying the adhesive.

2.3 Dispersion of GNPs inepoxy resin

As reported in the earlier study[5] andcan be seen in **Figure 1**, epoxy resincontaining 0.2 wt% weight percentage of GNPs had a superior mechanical properties in comparison with other GNPs contents of 0.1, 0.2 and 0.4 wt%.According to thisresult, in the current research, the incorporation of 0.2 wt% GNPs is used to modify the composite and FML panels.The incorporationinvolves the following six steps: (1)The GNPs are incorporated to epoxy without the use of solvents and then mixed by a high shear-mixer for 20 min at 2000 rpm. (2)For better dispersion, exfoliation and preventing agglomeration of GNPs, an ultrasonic mixer (UPS400S, Hielscher, Germany) at amplitude = 70% is employed for 13 min. In this step, the mixture is submerged in an ice bath to prevent overheating and aggregation [45]. (3) The shear-mixer is used once again for 15 min at 500 rpm. (4)To remove voids (air bubbles) created in the resin during the mixing process, the mixture is degassed for 15 min under vacuum (WOV-30 Precise Vacuum Oven, WiseVen, South Korea). (5) At the weight ratio of 100:13, the resin and hardener are mixed. (6) To eliminate voids, again, the mixture is degassed for 5 min under vacuum.It is noteworthy that all these processes areconducted at room temperature.A schematic of the preparation process is displayed in **Figure 2**.

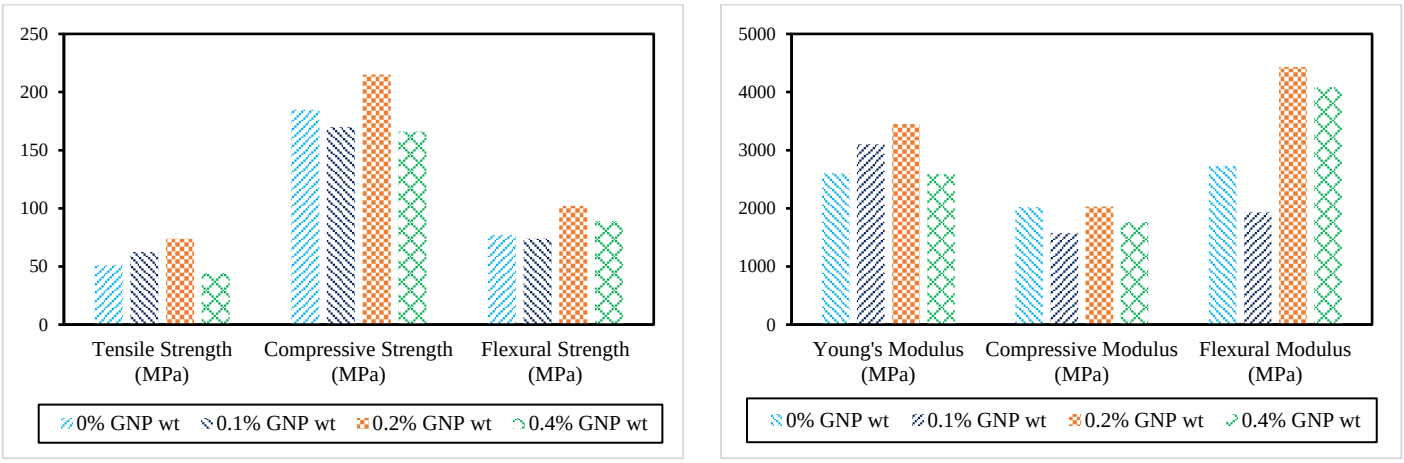

(a) (b)

Figure 1. The mechanical behavior comparison of epoxy resin with different percentages of GNPs in tensile, compressive and flexural tests: (a) comparison of strength; (b) comparison of modulus[5].

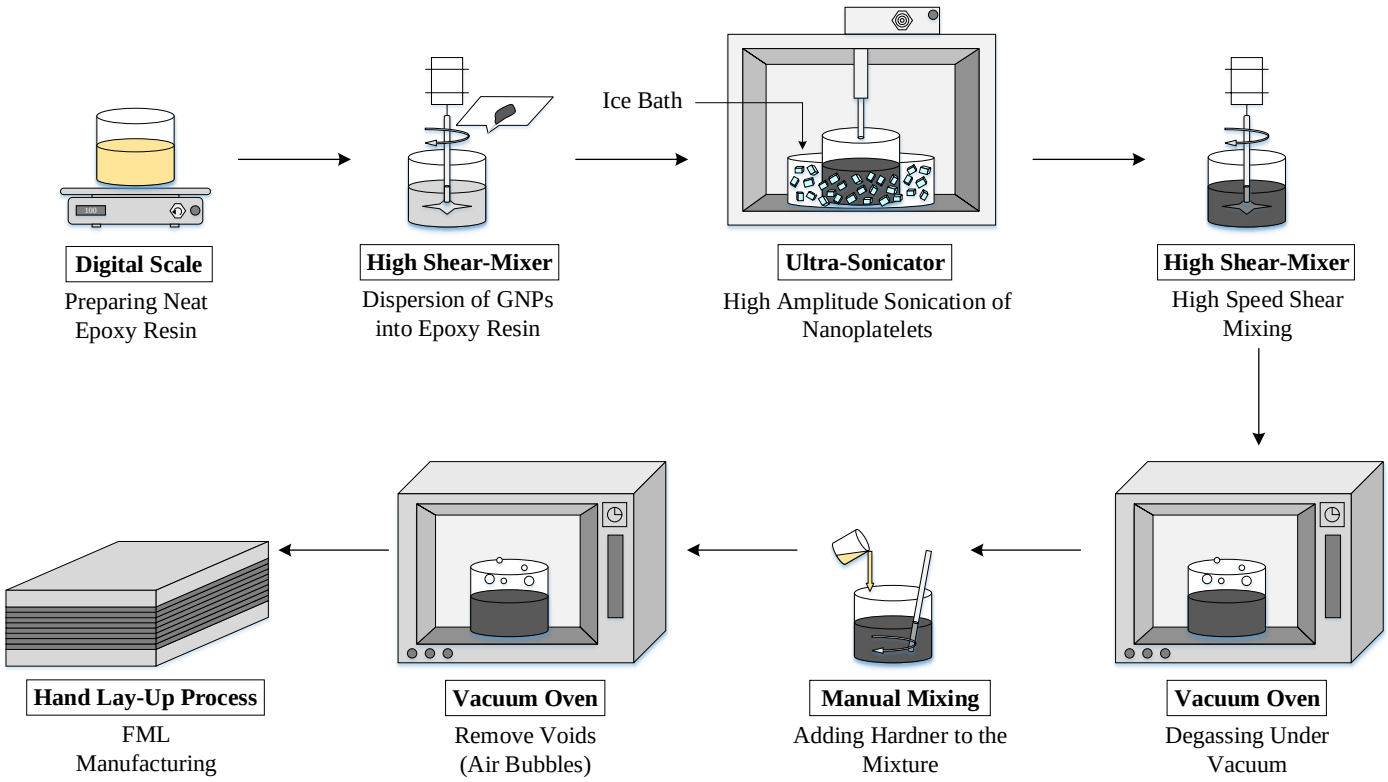

Figure 2. Schematic diagram of modified epoxy preparation.

2.4 Fabrication andspecimen preparation

The unreinforced and reinforced composite and FML specimensare manufactured in order to examine the effect of incorporation of GNPs on thelow-velocity impact behavior. The FML panelsare fabricated by hand lay-up technique with eight layers of glass fiber and two sheets of aluminum providing the stacking sequence of (AL/[G/E]$_8$/AL). Schematics of the FMLs fabrication are shown in**Figure 3**. The lay-up configuration of composite panels is [G/E]$_8$, which is identical to the composite laminate in the FMLs.The fabricated composites and FMLs are square with a width of 125 mm and the average thickness of 1.51 mm and 2.65 mm,respectively. After hand lay-up process, the panelsare pressed under 1.5 bar pressure[82] and the time duration between the fabrication of specimens and impact tests has been at least a week [83].All the manufacturing processes areaccomplished at room temperature.

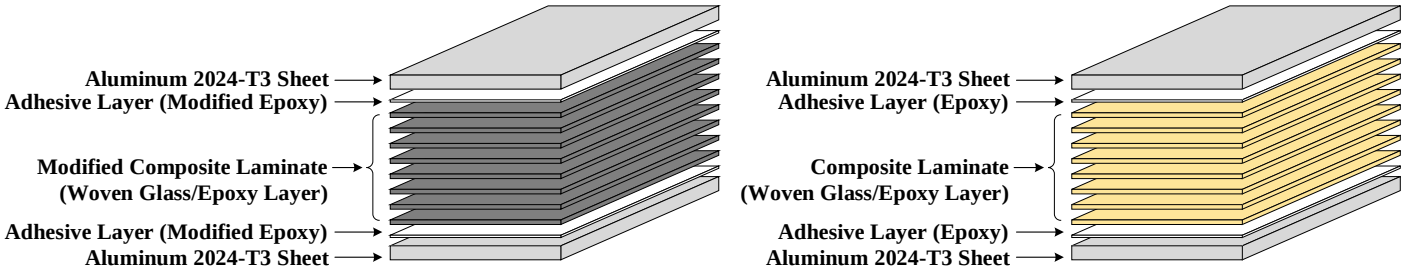

Figure 3. Lay-up configuration of FML panels.

2.5 Experimental method

Low-velocity impact behavior of the composite and FMLpanels is investigated using a drop-weight apparatus,as shownin **Figure 4**(a). The square panels with dimensions of 125 mm × 125 mmare fully clamped by a fixture with internal dimensions of 100 mm × 100mm and a span ratio (the ratio of support span length to the impactor diameter) of 10. The samples are fixed by a mechanical clamping system that ensures uniform pressure throughout the clamping area. The fixture is clamped by eight M16 bolts, steel nuts and washers, and also in order to prevent slippage of the specimen during the test,two M8 bolts are used to fasten the fixture to the testing machine.A schematic drawing of the panel and the clamp are displayed in**Figure 4**(b).

Prior to impact test, in the previous work of the authors [5], quasi-static indentation testswere conducted to obtain the required information regarding energy absorption characteristics of specimens, which can serve as a starting point for deciding on energy levels in impact testing.Therefore, by altering the height of the impactor, three different impact energy of 33J, 44J and 82 J areapplied at room temperature on unreinforced and reinforced specimens.The steel impactor used in the tests is a flat-ended cylinder with a 10 mm diameterand 6kg weight.

In order to ensure the repeatability of the results, minimum of three samples are tested at each energy level for each sample type. The output of the low-velocity impact test is represented as acceleration versus time.To measure it, a piezoelectric accelerometer is mounted on the impactor and the signal is acquired at 96 kHz.The deflection history is obtained by taking into account the energy balance equation during the impact. To do this,

the acceleration history is integrated numerically twice over time, considering the initial value of the velocity.Finally, the absorbed energy history, which represented the history of energy transferred from the impactor to the specimens, is obtained via an additional integration of the load with respect to the deflection. It should be mentioned that for non-perforated FMLs, ultimate damage of panels has been compared and presented curves are corresponding to the first hit of impact.

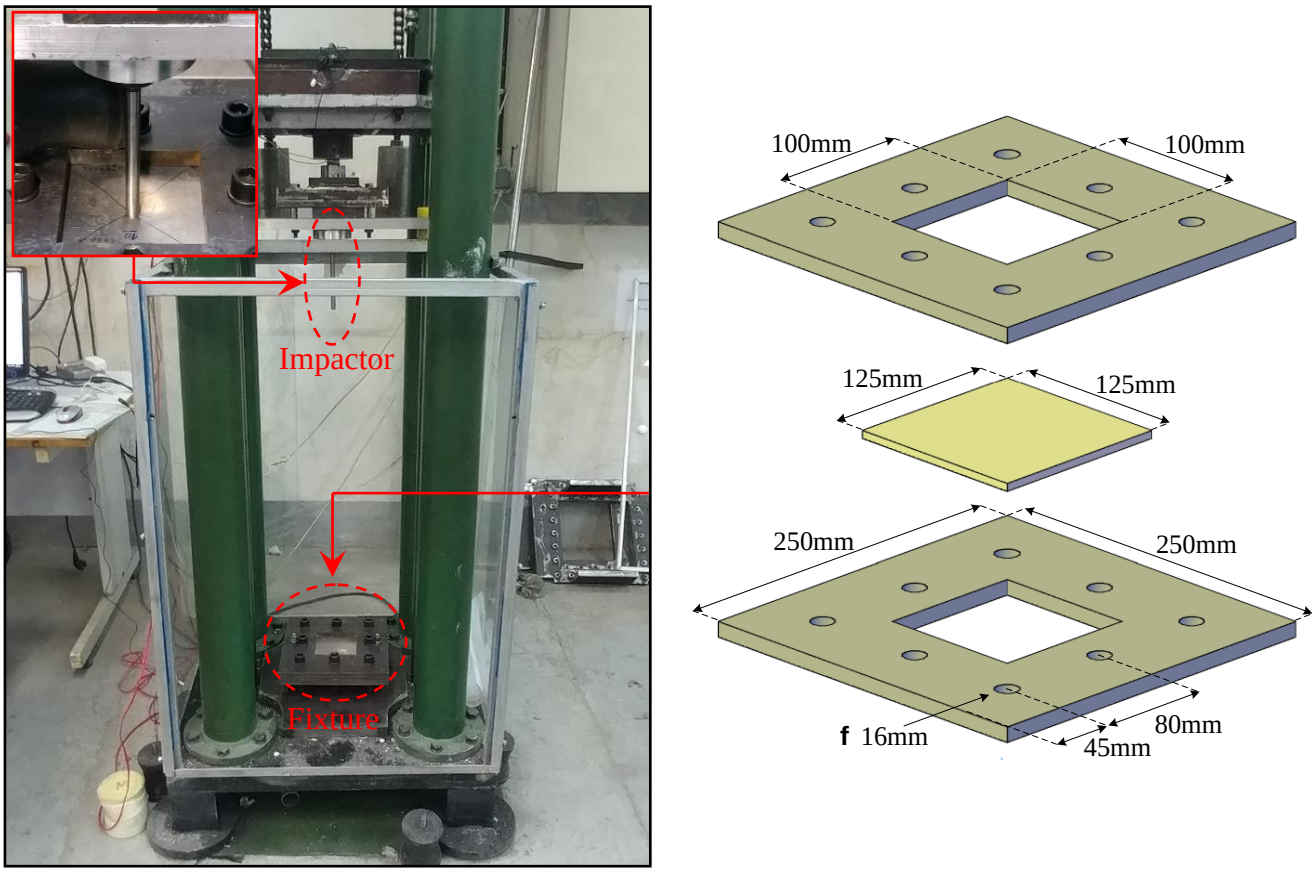

(a) (b)

Figure 4.(a) Fixture installation on the drop-weight apparatus; (b) schematic of fixture

3 Results and discussion

The low-velocity impact testsare performed on the unreinforced and reinforced specimens, in order to investigate the effect of adding GNPs. The results are presented, and discussed in detail in the following sections.In addition, to examine the influence of strain rate on performance properties of specimens,the results corresponding to impact tests are compared with those observed for identical panels subjected to quasi-static

test reported in our previous work[5]. The observations obtained from the visual inspection of testedspecimens are summarized in **Table 2**.

Table 2. Summary of the quasi-static indentation andthe low-velocity impact results.

Test	Specimens	Penetration Situation	Damage
Indentation	Unmodified Composite	Perforated	Fiber Failure/Bending, Matrix Breakage, Delamination
	Modified Composite	Perforated	Fiber Failure/ Bending, Matrix Breakage, Delamination
	Unmodified FML	Perforated	Debonding, Circular crack, Fiber Bending/Breakage, AL Bending
	Modified FML	Perforated	Debonding, Circular crack, Fiber Bending/Breakage, AL Bending
33 J Impact	Unmodified Composite	Perforated	Fiber Failure/Pull Out, Matrix Breakage, Delamination, Shear plugging
	Modified Composite	Perforated	Fiber Failure/Pull Out, Matrix Breakage, Delamination
	Unmodified FML	Partial Indentation	Indentation, Plastic deformation, Bulging
	Modified FML	Slight Indentation	Slight Indentation, Bulging
44 J Impact	Unmodified FML	Perforated	Circular crack, Fiber Bending/Breakage, AL Bending/Cracking/Petalling
	Modified FML	Partial Indentation	Slight Indentation, Localized Plastic Deformation, Bulging
82 J Impact	Unmodified FML	Perforated	Circular crack, Fiber Bending/Breakage, AL Bending/Cracking/Petalling
	Modified FML	Perforated	Circular crack, Fiber Bending/Breakage, AL Bending/Cracking/Petalling

3.1 X-ray-diffraction analysis

A comparative investigation on X-ray-diffraction (XRD) spectra of the GNPs, the neat epoxy resin and the GNPs/epoxy nanocomposite can demonstrate the quality of GNPs dispersion. As illustrated in **Figure 5**(a), the XRD spectra of GNPs exhibits a sharp diffraction peak at $2\theta = 31^{o}$ and two weak peaks at $2\theta = 51^{o}$and 64^{o}, which is in good agreement with the results given in[84].It is noteworthy that in this study the different X-ray source (Cobalt, $\lambda CoK\alpha 1 = 1.789$ Å) is employed, leading to a slight shift of the peaks detected in comparison with the ones reported inliteratures that use a Cu target [68,72,85].The XRD pattern of a pure substance can be described as an identification of that, because the same material always gives the same pattern [72].In general, the disappearance of characteristics peaks of GNPs in XRD patterns of nanocomposites would indicate that nanoparticles are uniformly dispersed within the matrix [86].The diffractograms of GNPs/epoxy nanocomposite, as displayed **Figure 5**(b), resembles very closely to the XRD spectra of the neat epoxy. In

addition, the peaks at 31° for GNPs cannot be observed for the modified epoxy, whichis an evidence of appropriate dispersion of GNPs.

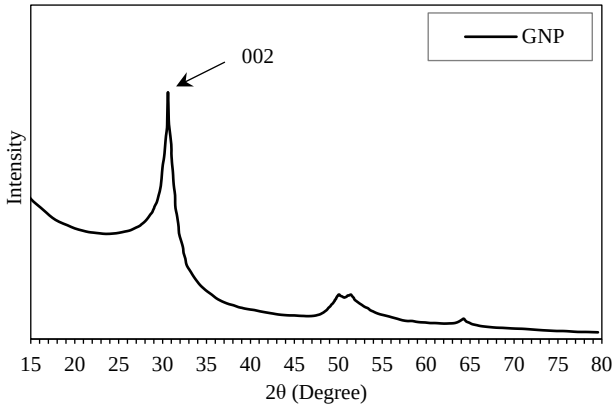

(a)

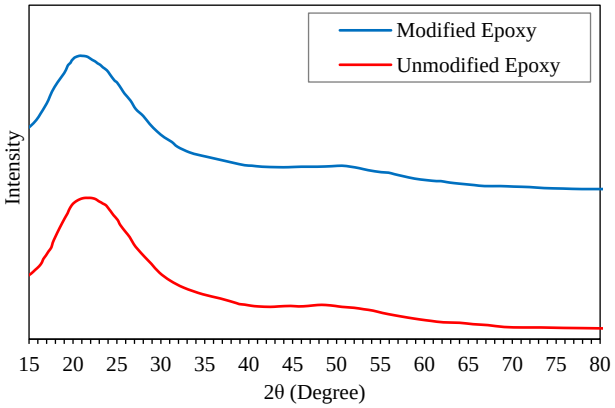

(b)

Figure 5.XRD patterns of: (a) GNPs;(b) unmodified and modified epoxy.

3.2 Quasi-static indentation test

Prior to impact tests, quasi-static indentation tests with a loading rate of5 mm/min were conducted on composite and FML panelsto obtain information regarding energy absorption characteristics of specimens, which can serve as a starting point for deciding on energy levels in impact testing.Sincethe present work can be considered as a continuation of the previous study, a summary of the results obtained in quasi-static test, which can be found in [5], is given in the following.It should be noted that panels investigated in low-velocity impact tests are identical to those in quasi-static loading.**Figure 6**illustrates the load-deflection curves of unmodified and modified panels under the quasi-static loading.The results show that an enhancement of 15.2% in peak load

and 31.2% in SEA are obtained by reinforcing composite panel. The reason for this improvement will be discussed in Subsection 3.6.5. As for FML curves, the first failure in the modified specimens is debonding between the aluminum and composite interface, which is accompanied by a rapid load-drop at 2.6 kN. Thus, owing to this reduction, the incorporating 0.2 wt% of GNPs into the FML decreases the peak load and does not have significant influence on the SEA. The resultant damage patterns of unmodified and modified FMLs can be observed from **Figure 7**, including a circular crack, matrix cracking, bending and breakage of the composite plies, bending, cracking and petalling of the bottom aluminum layer.

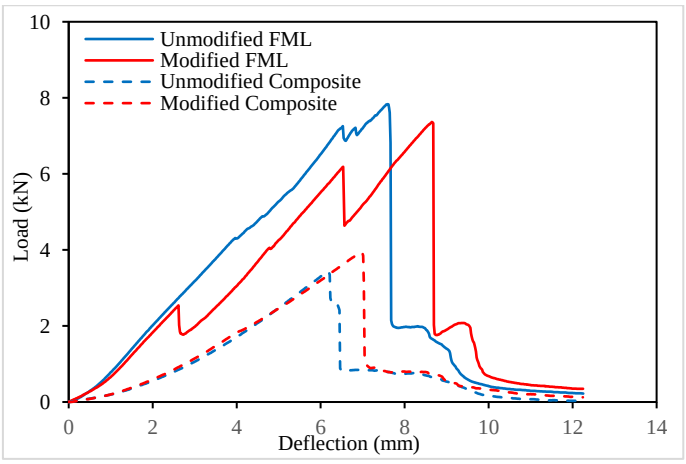

Figure 6. Load–deflection curves of composite and FML panels under quasi-static loading[5].

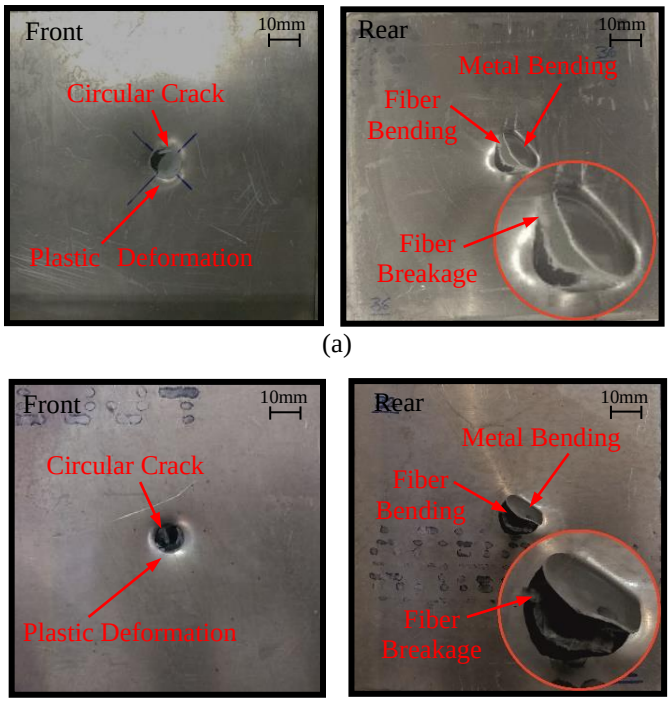

(b)

Figure 7. Damage morphologies of FMLs subjected to quasi-static loading: (a) unmodified panel; (b) modified panel [5].

(Magnification of damaged area is denoted by the circle)

3.3 Experimental testing under 33 J impact energy

In 33J impact energy event, to get a clear outcome on the influence of incorporation of GNPs and investigatethe damage propagation modes in composite laminate of FMLs, unmodified and modified composite specimensare also tested.

3.3.1 Composite panels subjected to 33J impact energy

The low-velocity impact test is conducted on the unreinforced and reinforced composite panels and the behavior of these specimens has been analyzed to investigate the effect ofinclusion of GNPs to epoxy resin.**Figure 8**compares various responses: the time-histories of energy absorption, central deflection, contact load and contact stiffness of the composite specimens corresponding to E=33 J impact energy.

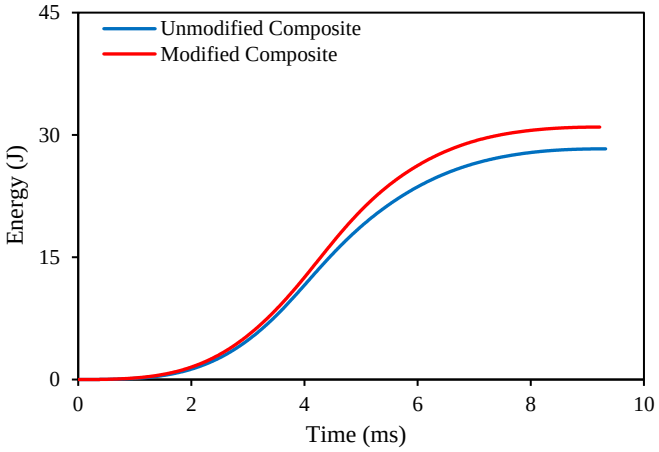

(a)

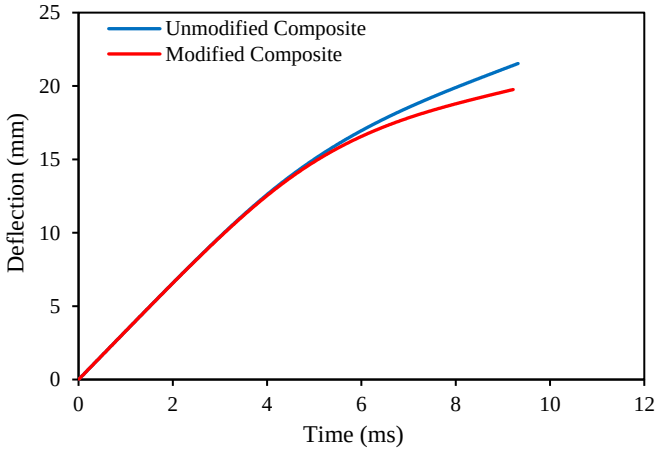

(b)

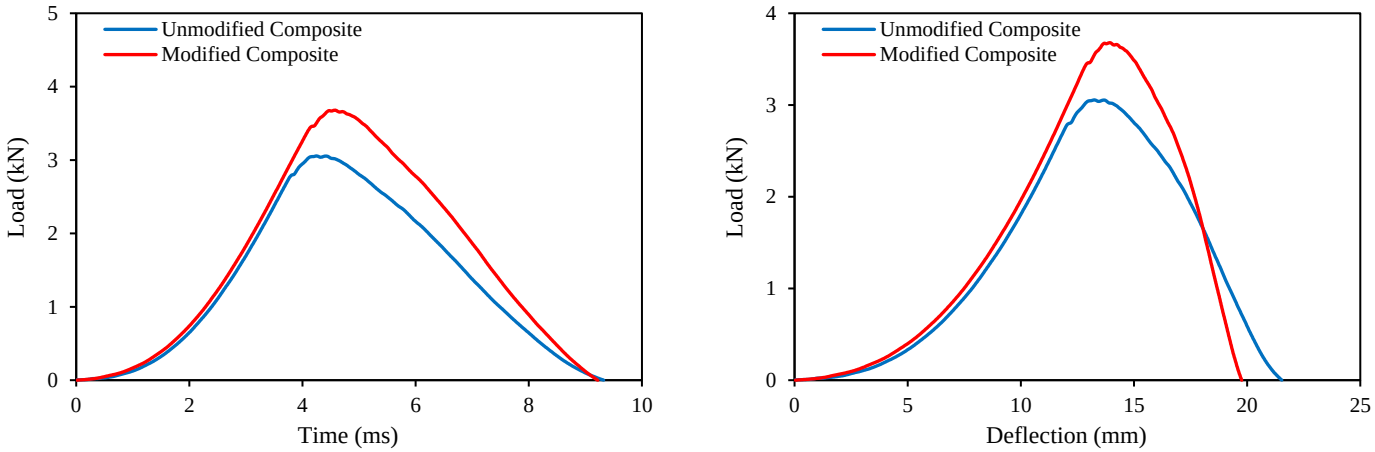

(c) (d)

Figure 8. Low-velocity impact response of unmodified and modified composite panels impacted at 33 J: (a) absorbed energy; (b) central deflection; (c) contact force; (d) contact stiffness.

As for the impact load-deflection curves, on the one hand, two curves havesimilar trends, which indicates that failure modes of specimens can be analogous. On the other hand, for the modified specimen the peak load occurs at higher displacement, therefore, the failure modes are delayed and this delay leads to more energy absorption and higher strength in comparison with the unmodified composite panel. As a result, the incorporation of GNPs to the composite panel increases the peak load, the energy absorption and the SEA by 21%, 10% and 11%, respectively.Likewise, Fathi et al. [5] stated that the GNPs inclusion can have significant effect on strength and energy absorption of composite panels which have undergone quasi-static punch and indentation tests. **Figure 9** exhibits the resultant damage patterns on the non-impacted and impacted sides of the unmodified and modified composite panels. As the figure indicates, both specimens are fully perforated. Moreover, diversified failure mechanisms including fiber failure, fiber pull out, matrix breakage and delamination between composite plies can be observed from the damage morphologies. The damage mechanisms in composite panels are similar except that the shear plugging occurs just in the unmodified composite, which implies that the effect of addition of GNPs on the failure modes cannot be neglected.

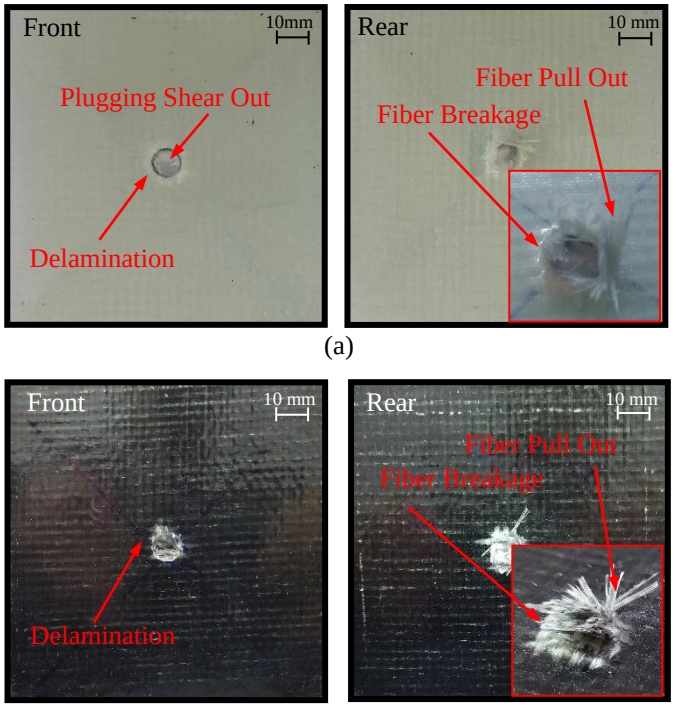

Figure 9. Damage morphologies ofcomposites subjected to 33J impact energy: (a) unmodified panel; (b) modified panel.

(Magnification of damaged area is denoted by the circle)

3.3.2 FML panels subjected to 33J impact energy

When the 33 J of impact energy is performed to examine the low-velocity behavior ofthe unmodified and modified FML panels, the time-histories of energy absorption, central deflection, contact load and contact stiffness are depicted in**Figure 10**.According tothe energy-time curves, it is well observed that the energy absorption increases with time until its peak,subsequently there is a reduction, which is corresponding toimpactor rebound during the impact process. This phenomenon can be explained in view of the fact thatthe impact energy of 33 J is not sufficient to make the impactor perforate the laminates. Generally, aload–deflection curve,which is the signature of a specimen's response to impact loading, can be classified as closed type curve and open type curve [6,87]. As for theload-deflection curves, both curves are closed type and consist of an ascending stage of loading, a peak load value and a descending stage of unloading.

In the loading phase,from the start of loading (point A) to point B,the curves of unmodified and modified FMLs have similar trend.Generally, the slope of the impact load-deflection curves increases monotonously until a

failure occurs in the specimen. From point B onward, as the impact load continuously increases, the slope of the load-deflection curve for the unmodified FML reduces, which implies that the unmodified FML experiences more serious damage in the loading stage. Subsequently, the peak load of reinforced FML increases by 12% in comparison with the unreinforced specimen.As displayed in the deflection-time curves (**Figure 10**), maximum deflection ofthe unreinforced FML is slightly higher than that ofthe reinforced one (point C), whereas ultimate central deflection of both laminates are almost the same (point D).

As discussed previously, no perforation occurs in any of the laminates, but according to **Figure 11**, the unmodified panel experiences more damage extent in the impact region. For unmodified FML, an indentation as well as plastic deformation of aluminum sheet around the impact point occurs, whereas for modified FML, only the slight indentation can be found on the impacted side and also the unmodified panel exhibits a greater bulge on the non-impacted side. In addition, regarding to **Figure 22**, an interfacial debonding occurs between the aluminum layers and the composite laminate, whereas there is no evident delamination between composite plies. The slighter damage of the reinforced FML can be attributed to the fact that the addition of GNPs has a remarkable influence on the impact resistance compared to unreinforced one.

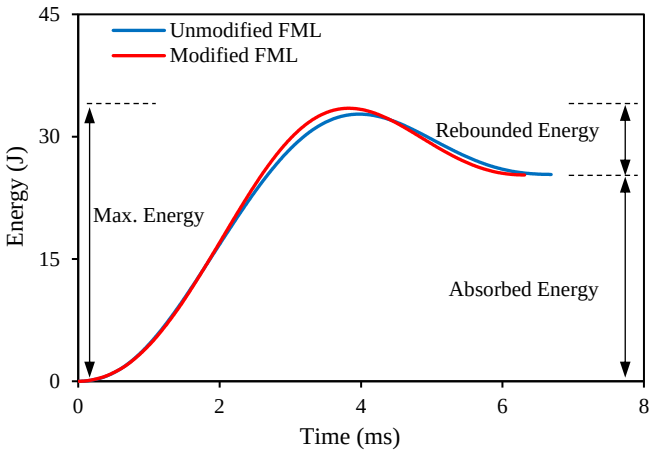

(a)

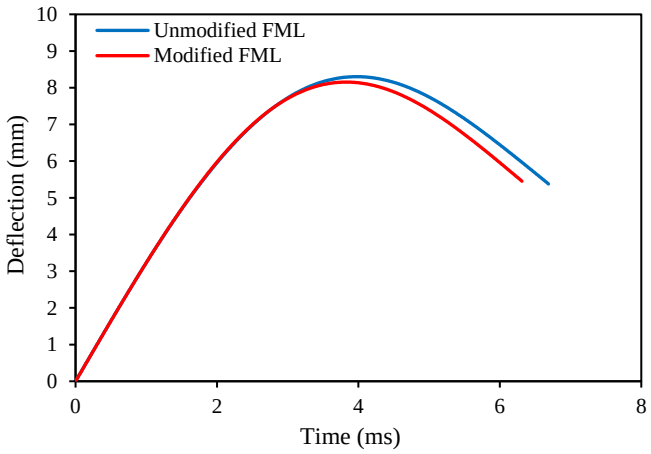

(b)

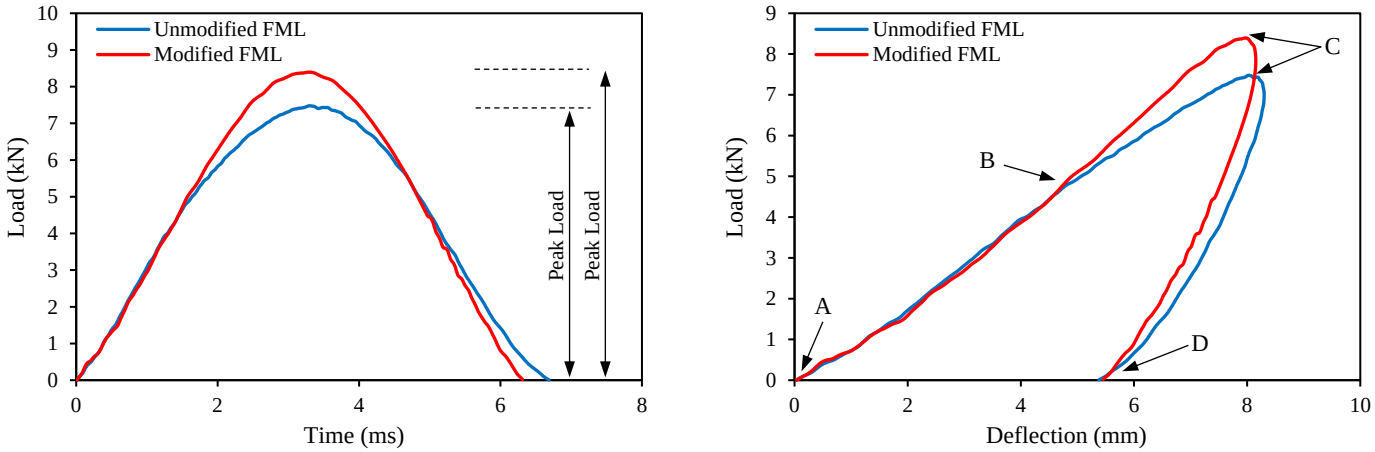

(c) (d)

Figure 10. Low-velocity impact response of unmodified and modified FML panels impacted at 33J: (a) absorbed energy; (b) central deflection; (c) contact force; (d) contact stiffness.

Consequently, since the modified laminate has higher strength, it exhibits the higher peak load and the lower contact-time duration. Additionally, in spite of the fact that both specimens absorb equal energy, the modified FML represents the better impact damage resistance than the unmodified FML due to the smaller damage area.

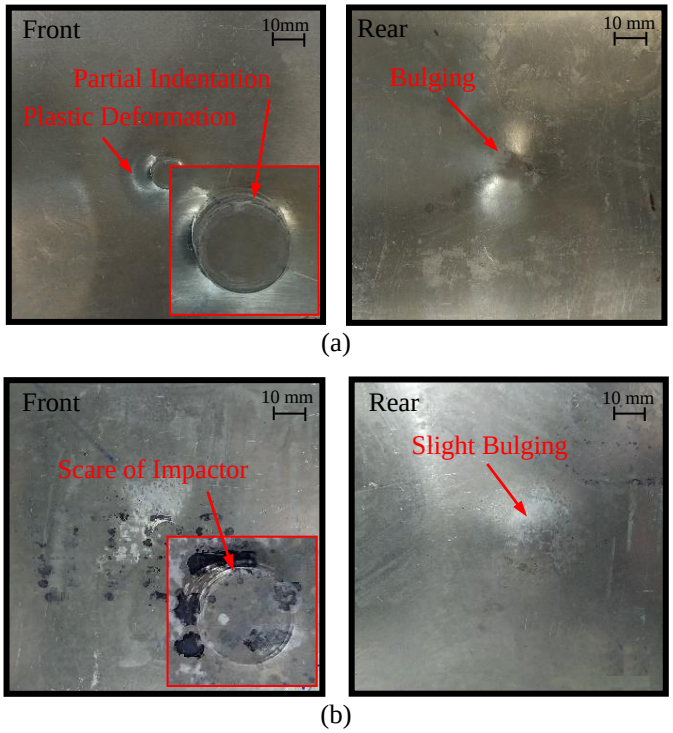

Figure 11. Damage morphologies ofFMLs subjected to 33J impact energy: (a) unmodified panel; (b) modified panel. (Magnification of damaged area is denoted by the circle)

3.4 FML panels subjected to 44J impact energy

Figure 12illustrates the time-histories of energy absorption, central deflection, contact force and contact stiffness of the unmodified and modified FML panels impacted with 44 J.As regards the energy-time curves, it can be observed that the energy absorption of the modified panel drastically reduces after the peak value, whereas the curve ofthe unmodified panel tends to be flat. It is in accordance with the fact thatthe impact energyof 44J is less than the energy required to penetrate the reinforced laminate and thereforeimpactor rebound is apparent in this specimen, while the unreinforced laminate is completely perforated. This phenomenon indicates that the inclusion of GNPs to epoxy resin has a great influence on the impact resistance of modified FML and increases the perforation threshold energy compared to the unmodifiedone.

As for load-deflection curves in **Figure 12**, the peak load of modified specimen is 5% higher than that ofthe unmodified one due to higher strength. Since the unreinforced FML is fully perforated while no penetration occurs in the reinforced panel, no comparison can be carried out in terms of absorbed energy, contact-time and maximum deflection.

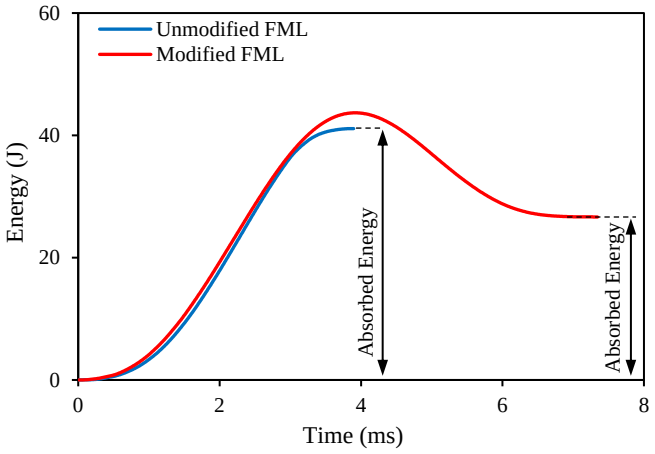

(a)

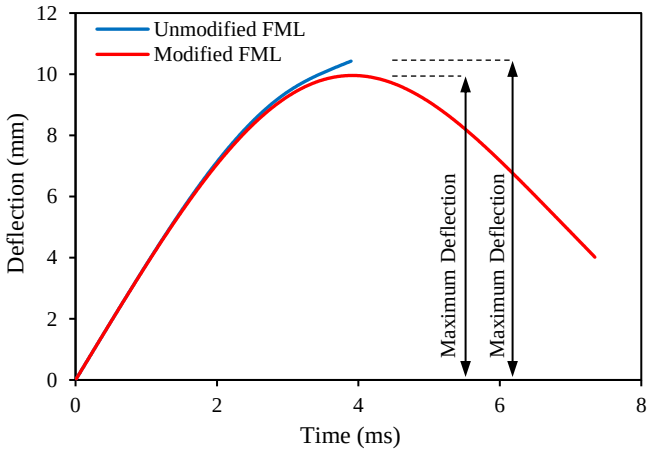

(b)

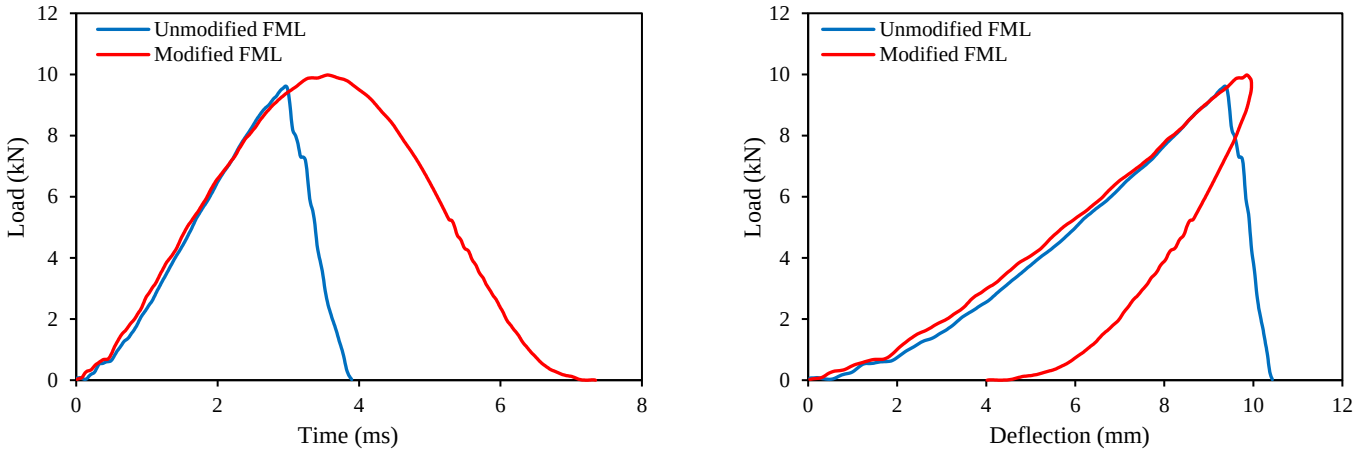

Figure 12. Low-velocity impact response of unmodified and modified FML panels impacted at 44 J: (a) absorbed energy; (b) central deflection; (c) contact force; (d) contact stiffness.

The post-impacted images of the front and rear surfaces of unmodified and modified FMLs are shown in **Figure 13**. As for the damage morphologies ofthe reinforced panel, the impactor does not perforate. In addition, on the impacted side of this laminate, only a small plastic deformation close to the perforation zone and a slight indentation on the aluminum layer can be observed, and on the non-impacted side, there is no obvious crack - just alocalized bulge can be found inthe impact region. On the contrary, the impactor fully perforates the unreinforced laminate and forms a circular crack in the top surface. Furthermore, on the non-impacted side, matrix cracking, bending and breakage of the composite plies and bending, cracking and petalling of the bottom aluminum layer can be seen obviously from the post-impacted images of this specimen. Thus, these results confirm that the incorporation of GNPs into the composite laminate of FML significantly improves the impactperformance of the modified panel in comparison with the unmodified one.

The perforation process in unreinforced panel can be explained in view of the fact that first,a shear plug with the diameter equal to the impactor is created in the uppermost aluminum layer. Then, the formed plug begin to be pushed through the composite laminate and create a petal in it. Finally, at the perforation threshold, the impactor passes through the entire panel leaving a relatively clean hole on the front surface and petalling at the rear surface. The similar phenomenon can also befound in [5,39,88].

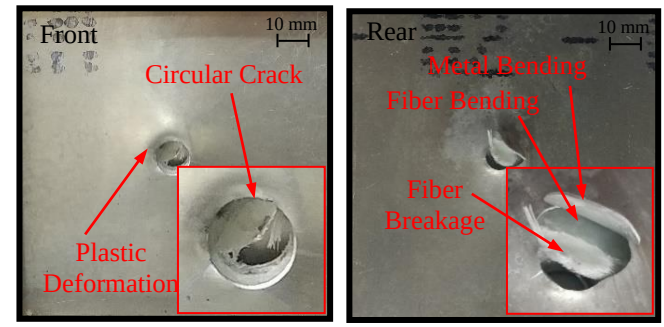

(a)

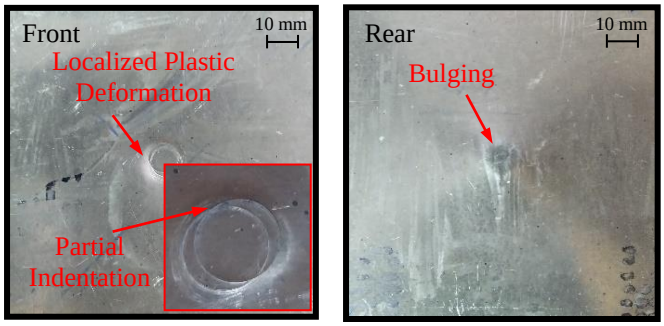

(b)

Figure 13. Damage morphologies ofFMLs subjected to 44J impact energy: (a) unmodified panel; (b) modified panel. (Magnification of damaged area is denoted by the circle)

3.5 FML panels subjected to 82J impact energy

In order toexaminethe effect ofthe incorporation of GNPs into FML on the impact behavior when impact energy is higher than the perforation threshold energy, the unreinforced and reinforced panels are tested under 82 J impact energy and results are exhibited in **Figure 14**.As the impact energy further increases (from 33J to 82J) the load–deflection curve type gradually changes from the closed type to the open one, similar behavior is also found in [6,87].

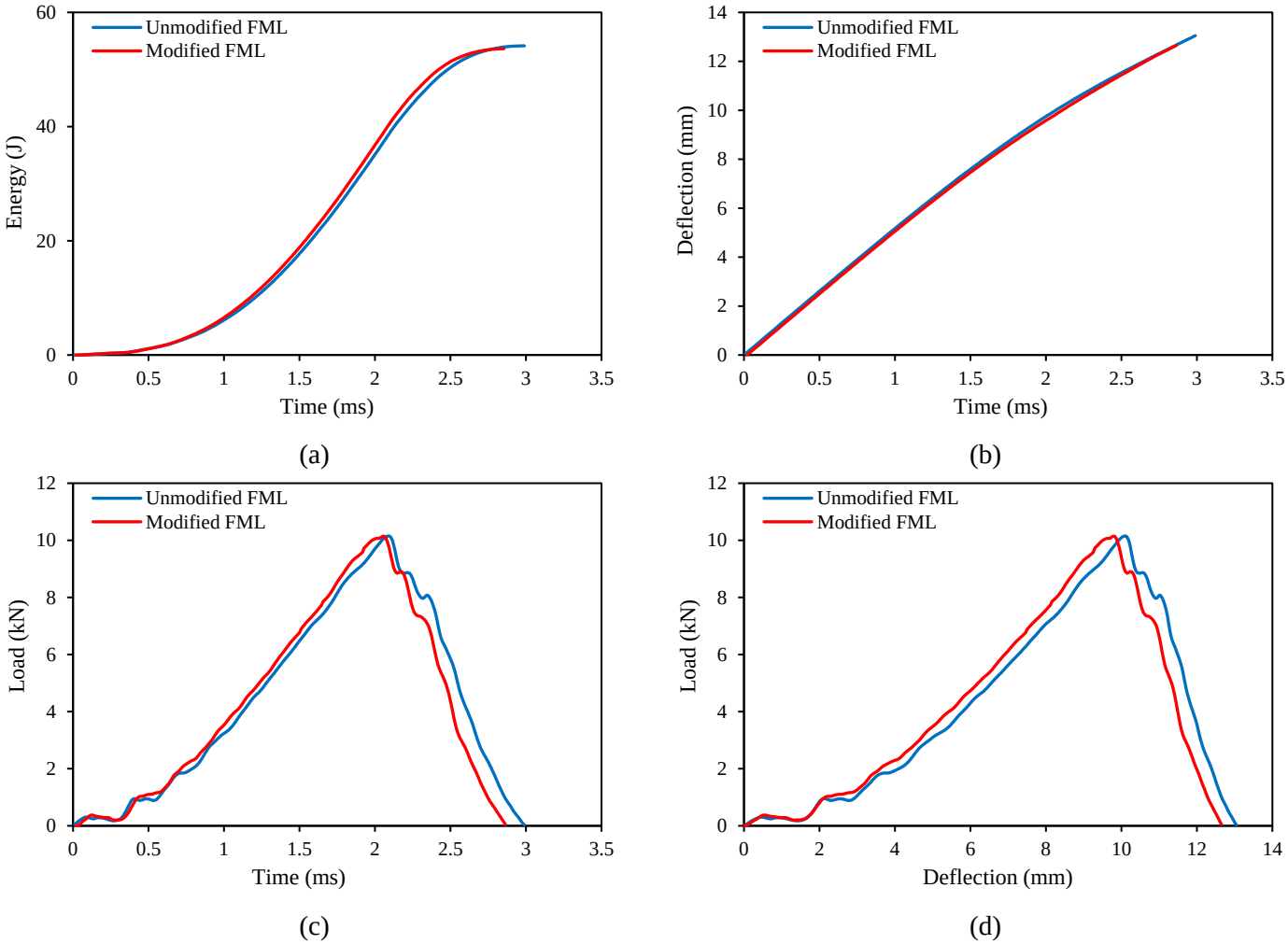

Figure 14. Low velocity impact response of unmodified and modified FML panels impacted at 82 J: (a) absorbed energy; (b) central deflection; (c) contact force; (d) contact stiffness.

At 82 J impact energy, the load–deflection curvesare open type and the energy-time curves always keep increasing, which indicates thatthis energy level issufficient to induce full perforation in both unmodified and modified specimens.The load-deflection curve of reinforced FML is virtually identical to that ofunreinforced one when subjected to low-velocity impact of 82 J.However, regarding to**Figure 15**, the plastic deformation area and metal cracks corresponding to the unreinforced FML is bigger than that of the reinforced FML. Additionally, the addition of GNPs decreasesthe contact-time duration and maximum deflection of reinforced panelin comparison with thoseofthe unreinforced one.The contact-time duration is correlated to the contact stiffness as well as the time of energy transfer to propagate damage in the specimen. Since the increase in the bendingstiffness of the modified panel is insignificant (**Figure 20**), shorter contact-time duration can indicate

less damage extent. Likewise, Seyed Yaghoubi et al. [29] stated that decreasing contact-time means that damage cannot be fully developed in the sample. Similar observation has also been reported by Yu et al. [6].

Moreover, a change in the slope ofthe load-deflection and load-time curves occurs several times. These fluctuations can be explained by the intensity and propagation of damage in specimens in different time intervals, which is also found by Ref [29]. As for **Figure 14**, the fluctuations in the curve of unmodified specimen are slightly more than thoseofthe modified one, which implies that more damage induces in this panel in comparison with the modified one.

The modified specimen exhibits damage modes similar to the consequences of impact on the unmodified one, except that the global plastic deformation and metal cracks in unreinforced panel are more than those in the reinforced one, as depicted in to **Figure 15**. Accordingly, lower damage extent in the reinforced FML indicates that the influence of incorporation of GNPs on the impact behavior of this panel cannotbe neglected. According to the damage morphologies (**Figure 15**) and the cross-section view of the modified FML (**Figure 22**), matrix cracking, bending and breakage of the composite plies, plastic deformation, cracking and petalling of aluminum sheets, debonding and delamination are the main failure modes of the panels.

As reported by Ahmadi et al.[89], for FML panel under high velocity impact, the most part of energy absorbing mechanism is the global deformation of the aluminum sheets. In addition, the global permanent deformation has an important role in dissipating energy, especially in thinner specimens [29]. It can therefore be concluded that at higher impact energies, the behavior of aluminum becomes moredominant and as a result, under 82 J impact energy, the incorporation of GNPs has less significant effect on the impact performance of the modified FML.

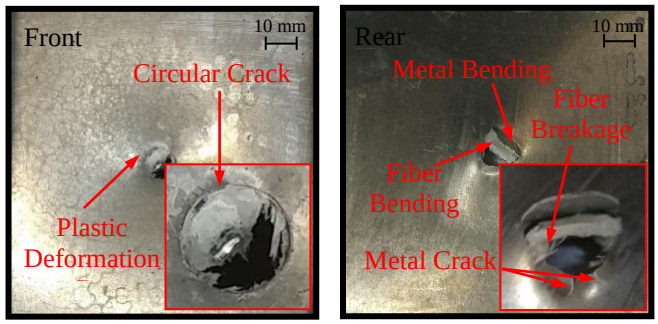

(a)

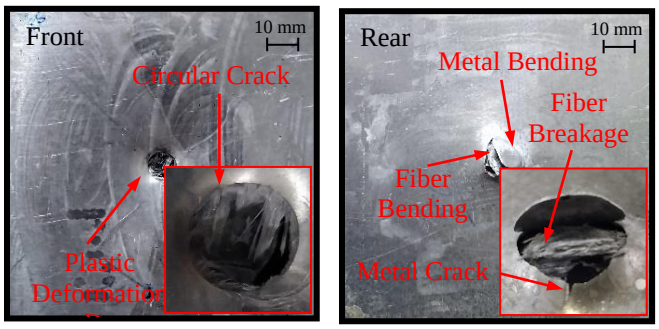

(b)

Figure 15. Damage morphologies ofFMLs subjected to 82J impact energy: (a) unmodified panel; (b) modified panel.

3.6 FML responses underdifferent loading rates

This section presents and discusses the quasi-static and low-velocity impact results with respect to strain rate effect, bending stiffness, coefficient of restitution and damage mechanisms.

3.6.1 Strain rate effect

The impact tests are performed subjected to varied impact energy levels including 33 J, 44 J and 82 J in order to investigate the impact response of the unmodified and modified specimens. In addition, the behavior of equivalent panels under quasi-static indentation loadingis compared with the impact performance of panels to examine the effect of strain rate. The generaltrend of the load-deflection curvesfor perforated panels in impact testsare virtually similar to quasi-static curves (**Figure 6** and **Figure 14**), which indicates that failure modes in these two test can be almost analogous.Furthermore, for the purpose of intuitive comparison, the key parameters in quasi-static and impact tests such as the absorbed energy, the SEA and the peak load are summarized in **Figure 16**.For the low-velocity impact tests, the maximum value of the energy absorbed in the

quasi-static loading is not sufficient to makethe impactor perforate the laminates, which implies that the perforation threshold energyis higher for both unmodified and modified panels at impact rates of loading. This phenomenon is attributed to the strain rate sensitivity of the constituent materials of FMLs and shows that the perforation resistance of the specimens can be enhanced by dynamic effects. On the other hand, there is an obvious difference between the behavior of FMLs under quasi-static loading and 33 J impact event, as depicted in**Figure 16**. For instance, FML specimens subjected to 33 J impact event absorb significantly less energy (-26%) than FMLs subjected toquasi-static loading.

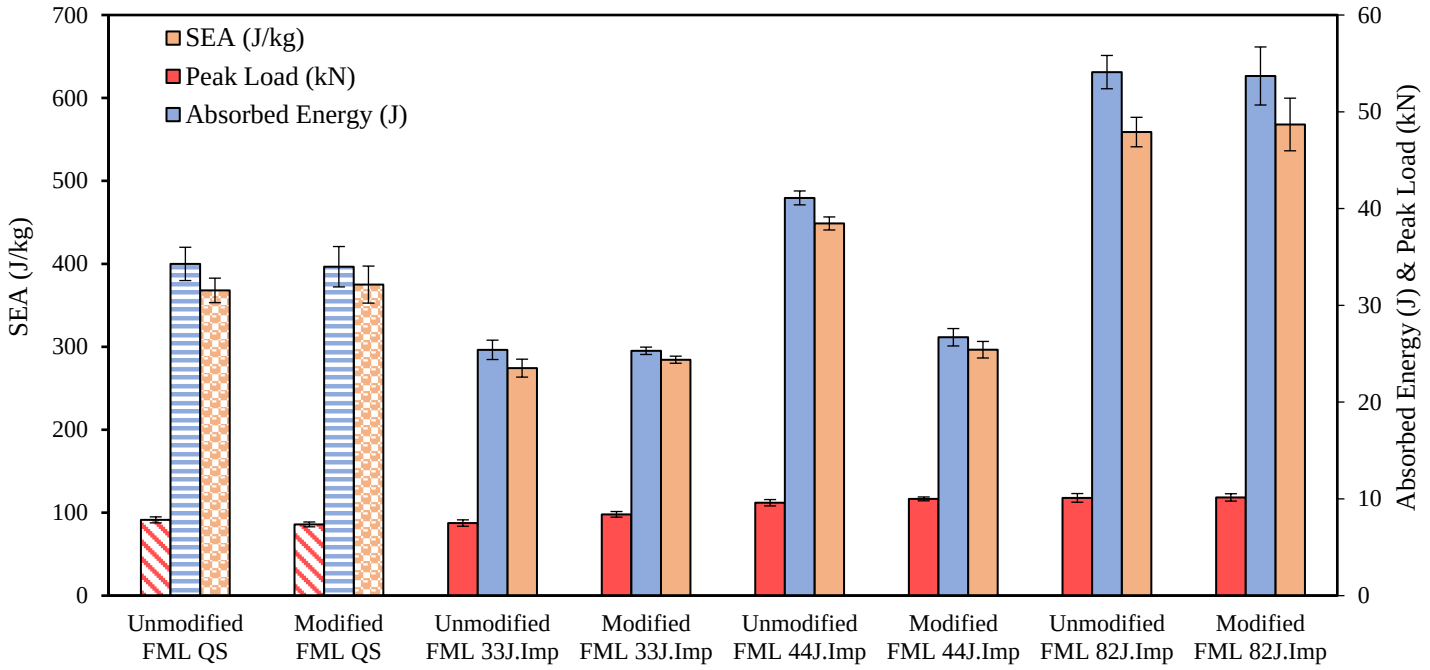

Figure 16. The comparison ofFML responses under different loading rates.

Moreover, as exhibited in **Figure 16**, when impact energy is higher than the perforation threshold, the peak load, the energy absorption and SEA are considerably greater at dynamic rates of loading in comparison with values obtained at the quasi-static rate of strain. As an example, the peak load of the modified panel under 44 J impact energy is 23% higher than that in quasi-static test, which shows that strength of the FML specimens can be enhanced by dynamic effects. Comparing failure modes of FMLs in the quasi-static loading (**Figure 7**) and dynamic test (**Figure 15**), damage mechanism are similar in these two tests, except that the impact test results in the more severe aluminum cracking and fiber pull out.

For dynamic tests, generally, increasing the impact energyleads to higher absorbed energy (see **Figure 16** and **Figure 17**), maximumdeflection (see **Figure 18**), peak load (see**Figure 19**), and lower contact-time duration (see **Figure 17**) for both specimen types, similar results have also been observed by Zarei et al.[90].These evidences highlight the strain rate sensitivity of the constituent materials of FMLs[36].As discussed before,the load–deflection curves alter from the closed type to the open one by increasing the impact energy. In addition, the curves exhibits a rather smooth behavior under the 33J ofimpact energy, whilethe behavior of the load-deflection curves gradually changes to more oscillatory behavior as the impact energy further increases (compare **Figure 10**(c) with **Figure 14**(c)), which indicates that the damages become more severe.

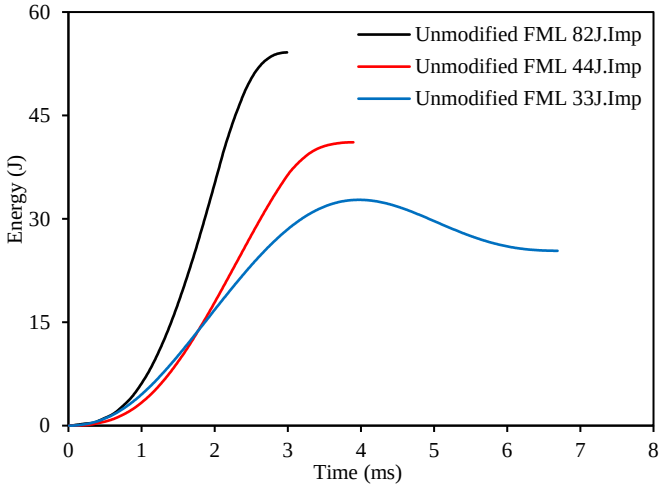

Figure 17. Absorbed energy-time curves of unmodified FMLs under different impact energies.

As depicted in **Figure 18** and **Figure 19**, by increasing the impact energy, on the one hand, the difference between the maximum deflection in the unmodified and modified FML increases. But on the other hand, the difference between the peak loads decreases. As mentioned earlier, the performance of unmodified and modified FMLs under 82 J impact energy is virtually similar and in spite of the fact that the addition of GNPs decreases the maximum deflection and contact time duration, it has an insignificant effect on the behavior of the modified under 82 J impact energy. It is noteworthy that, the maximum deflection in all modified FMLs is

less than that in unmodified ones. Moreover, when the impact energy increases from 33 J to 44 J, the peak load of both specimens enhances considerably (see **Figure 19**). Whereas by further increasing the energy level (from 44 J to 82 J), improvement of the peak load is less significant. It can be concluded that there is a limit value of impact energy that would not result in further increase of peak load despite of further increase of this energy.

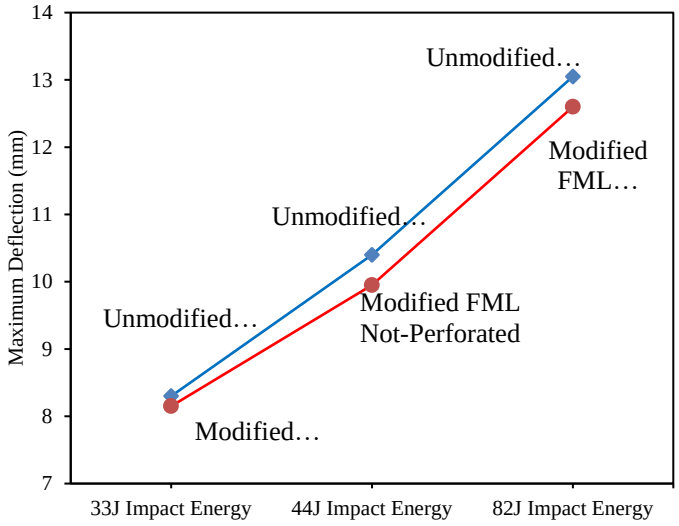

Figure 18. Maximum deflection in tested specimens under different impact energies.

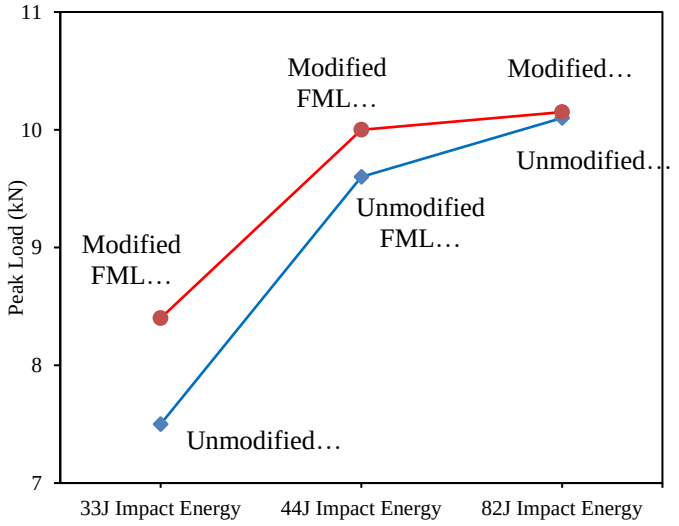

Figure 19. Maximum impact energies of tested specimens under different impact energies.

3.6.2 Bending stiffness

Bending stiffness may be employed as one of the quantitative criteria for assessing the specimens impact resistance due to its representation of the stiffness of laminates under impact-induced bending, which can be defined as the initial bend angle of a rectilinear section of load increase as a function of displacement [27].**Figure 20**illustrates determined ‘impact bending stiffness’ values of unmodified and modified laminates. It can be observed that the specimen stiffness is not constant at different impact energies, which demonstrate a strain-rate dependency of the stiffness, similar results also have been observed by Belingardi et al.[38]. In addition, as stated by Jakubczak et al.[15], this material property is contingent mostly on its thickness, component type and other structural features of laminates,andincreases along with a rise in energy impact.

As can be seen in **Figure 20**, the incorporation of GNPs results in the increase bending stiffness of composite and FML specimens in general. For instance, at 33 J impact energy, the contact stiffness of reinforcedcomposite and FML specimens was improved by 17% and 12%, respectively, compared to the unreinforced laminates. Moreover, it is reported that the inclusion of nanoparticles like MWCNTs [3], nanoclay [61], and pristine GNPs (PG) [78] can enhance the impact bending stiffness of composites and FMLs. It should be pointed out thatat the higher impact energy level (i.e. energy levels causing perforation), the increase in the stiffness of modified panels is less noticeable.

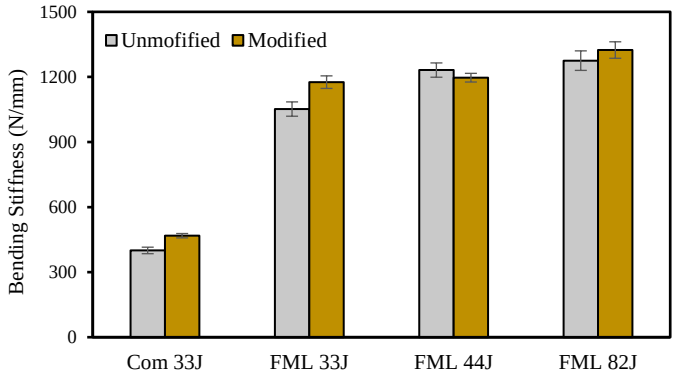

Figure 20. Bending stiffness of tested specimens under different impact energies.

3.6.3 Coefficient of restitution

In general the collision between the impactor and the FML is inelastic; thus, the interaction forces between the colliding bodies are non-conservative and some energy is lost during loading and unloading. It is expected that the amount of absorbed energy could serve as an indicator to the extent of damage in the low velocity impact[40].On the other hand, the coefficient of restitution (COR) can be arepresentation of material's capacity to absorb energy, which is often used for the quantitative assessment of impactresults. Although the comparison on the basis of COR only, hasproven to be insufficient, it can be used to some extent to compare the investigated FMLs[19].The COR is calculated as the ratio of the velocity of the impactor before and afterimpact[91]:

$$COR = \frac{V_{rebound}}{V_{impact}} \quad (1)$$

When COR = 1,the collision of impactor and laminate is completely elastic, while COR = 0 designates that 100% of the impact energy has been transferred to the panel. The above equation can be defined in terms of absorbed and impact energies as:

$$COR = \sqrt{1 - \frac{E_{absorbed}}{E_{impact}}} \quad (2)$$

Figure 21displays COR profiles of the unreinforced and reinforced laminates against the different impact energies.At 33 J and 82 J impact energy, the COR value is approximately equal for the unmodified and modified FMLs, which indicates that the incorporation of GNPs does not have significant influence on theenergy absorption capacity.When consideration of COR is applied so as to compare impactresistance, the most essentialmatter is the perforation observation of each specimen. The impactor velocity at impact can be similar to that when the impactor is rebounded and repelled. Nevertheless, in the above phenomena, the impact behavior of sample is different. This is the reason that totally perforated specimens cannot be compared by COR with non-totally perforated laminates[20]. Hence,at 44 J impact energy, since the unreinforced FML is

fully perforated while no penetration occurs in the reinforced panel, no comparison can be carried out in term of COR.

As for the unmodified curve, at relatively low impact energies (the perforation threshold energy or less), increasing the value of the impact energy produces a reduction in the COR value. The similar phenomenon can also befound in [19,20,91,92].In addition, as can be seen in Figure 21 and also stated by Sadighi et al. [19], increasing the impact energy further (from 44 J to 82J), results in an increase of the COR indicating that not all the energy is absorbed, which means the specimen is perforated.

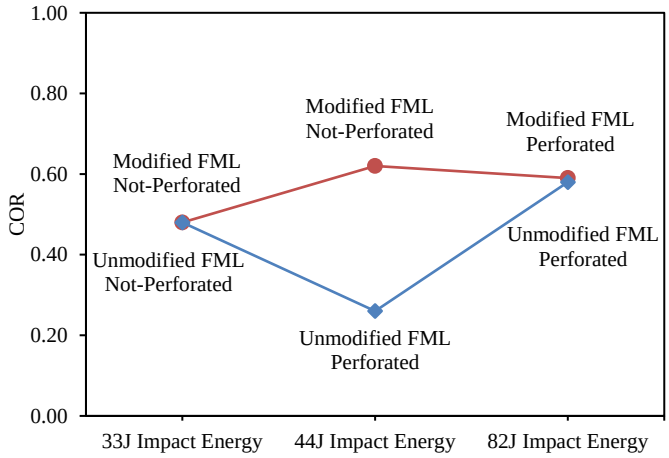

Figure 21.COR curves for the tested FMLs under different impact energies.

3.6.4 Damage assessment

Damage mechanism is an essential criterion in evaluation of composite and FML structures resistance to impact [26]. Investigation of damage mechanisms using cross-sectional views, corresponding CR and X-CT results are demonstrated for FML specimens in **Figure 22**. In addition, breakage, debonding and total damage area of the specimens are individually calculated and given in **Figure 23**.Considering specimens subjected to the quasi-static loading, damage pattern of the two panels are similar except that the debonding area, fiber breakage and metal bending in the unmodified FML expand broader than that in the modified one.For the unreinforced specimen under 33 J impact event, there is an indentation in the upper aluminum layer, and the debonding and

bulging area are wider compared to the reinforced panel. In addition, permanent deformation of the rear aluminum layer in unmodified FML (at 33 J impact energy) is considerably higher than that in modified specimens (at 33 J and 44 J impact energy), which indicates that GNPs incorporation significantly decreased the damage extent.

By looking at the cross-sectional view of the GNPs-modified specimens subjected to 33 J and 44 J impact energy,at44 J impact event the delamination and bulging area enlarge more widely. The conclusions can be drawn that the size of impact damage area increases with the increasing of impact energy irrespective of the constitution of FMLs [1].Moreover, it can be observed that localized plastic deformation of metal layers and the debonding between aluminum layers and composite laminate are the main damage under the lower impact energies, whereas global plastic deformation of metal layers, metal cracking, fiber fracture and delamination in composite plies transfer to the main damages at the higher impact energies.

As regards for **Figure 23**(a) and the CR results, when the specimens are fully perforated, neither the inclusion of GNPs nor the strain rate has significant effect on the breakage area of FMLs. Conversely, by comparing the debonding area (**Figure 23**(b) and the X-CT results) the modified specimens are characterized by considerably smaller debonding area in comparison to the unmodified laminates. As an example, in quasi-static indentation, the incorporation of GNPs reduces the breakage and the debonding area of the FML panel by 5% and 36%, respectively. Moreover, the GNPs inclusion is found to be more effective at the energy levels that caused no perforation, hence at 33 J impact energy, a reduction of 71% in the debonding area of the modified panel is obtained, in comparison to that of the unmodified panel. Likewise, some researchers stated that nanoparticle inclusion can substantially reduce the damage area of composites and FMLs[43,61,78,90].The analysis of the total damage area (**Figure 23**(c)) indicates that increasing impact energy is accompanied by increasing FML damage area. Similar results have been recorded in other works [26,41,93,94]. Furthermore, another study [13] proved that the delamination damage on the aluminum-composite interface is greatly affected by impact energy.

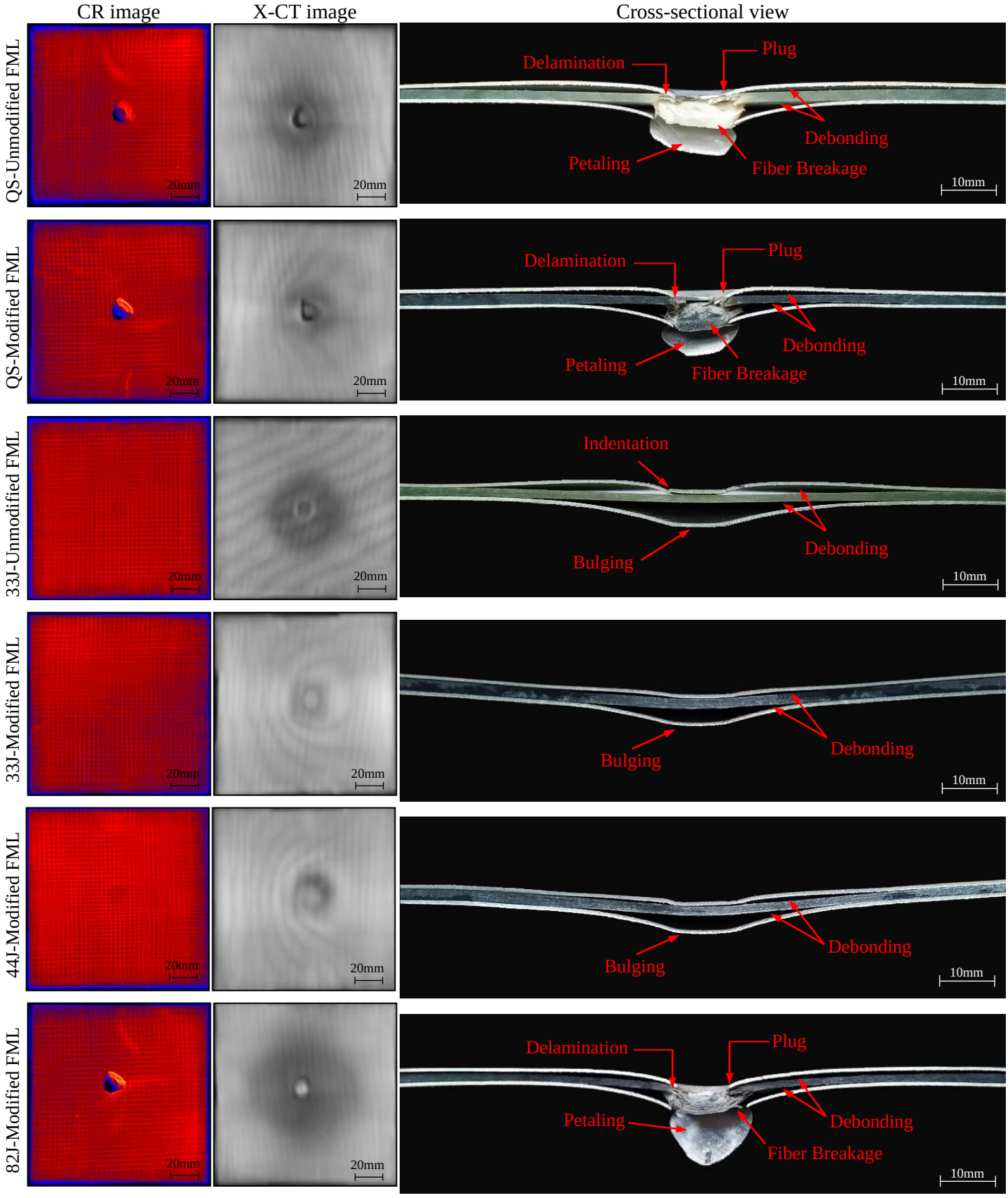

Figure 22.CR and X-CT results and corresponding cross-sectional viewof tested FMLs.

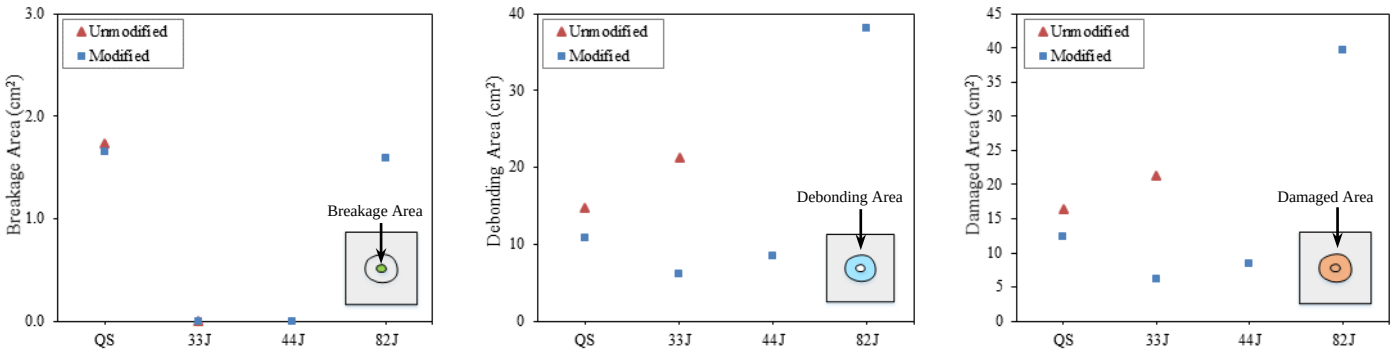

(a) (b) (c)

Figure 23. (a) Breakage (b) Debonding and (c) Total damage areas of the FML panels.

3.6.5 Microscopic observation

The adhesion interface of GNPs-modified FMLs between aluminum layers and composite laminate as well as composite plies aredisplayed in**Figure 24**. It can be observed that the two interfaces are combined well. As mentioned earlier, surface treatment of aluminum sheets increases the roughness of the aluminum surface, which in turn increases the surface energy of the substrate and provides mechanical interlocking, thereby enhancing the bonding strength[49,95].

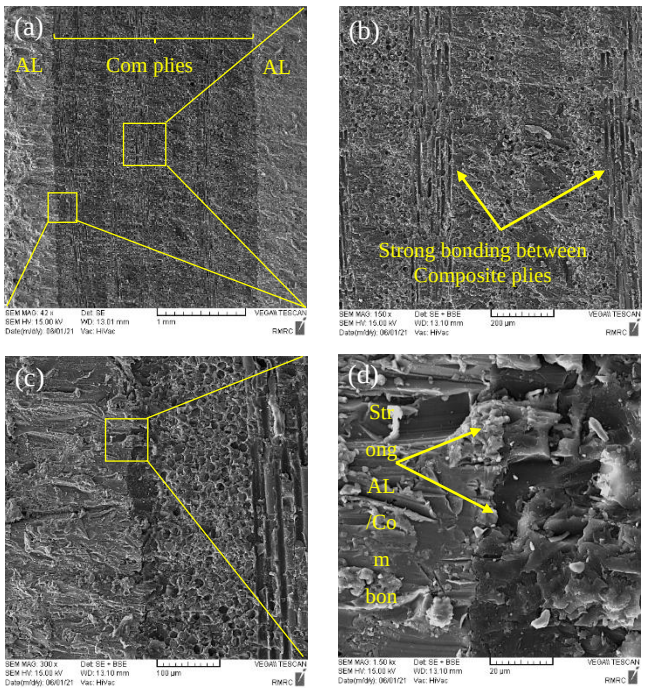

Figure 24. SEM images of Modified FML before impact: (a) over-view of sectional region; (b) close view of composite region; (c) and (d) close view of aluminum/composite bonding

The SEM images of the unreinforced and reinforced FMLs under different loading rates taken at the damaged areas areillustrated in **Figure 25** and **Figure 26**to further investigate the damage mechanisms.By comparing SEM results of unmodified and modified FMLs subjected to 33 J impact energy, as seen in **Figure 25**(a), the unmodified panel experiences more delamination extent, indicating poor adhesion between composite plies compared to the modifiedone.Thus, incorporating GNPs into the FMLs improves the adhesion between the composite layers and accordingly reducesdelamination area.Regarding to **Figure 25**(b) and (c) for 33 J impact event, in the unreinforced panel, owing to the weak interfacial adhesion between resin and glass fibers, most of the fibers are detached from matrix, and matrix cracks of this specimen are more severe. Moreover, an extensive cavity happened between composite plies of the unmodified panel, whichconfirms weak bonding between glass fibers and neat matrix. Whereas, in the reinforced FML, the modified matrixis perfectly bonded to glass fibers representing the enhanced adhesion between the resin and fibers in comparison with the unmodifiedone. Similar results have been observed in other works[43,52,77,96].The strong interfacial bonding is favorable to improve the stress transfer capacity from matrix to fibers and thus significantlyenhances the strength of specimens, which has been reported in previous researches[46,49,56,70]. Consequently, the inclusion of GNPs in composite laminate of FMLs increases the strength of this panelsand the improved impact resistance of GNPs-modified FMLs is mainly attributed to these micro damage mechanisms.

Under quasi-static loading, the SEM study for the fractured FMLs (**Figure 26**(a)-(d)) reveals a substantial improvement in the matrix and glass fibers interface adhesion as well asreduction inmatrix cracking, fiber breakage, fiber pull-out and debonding due to the addition of GNPs. This makes the damaged area of reinforced panelsreduce compared to the unreinforced specimens. As illustrated in **Figure 26**(c) and (g), for the unmodified panel, the smooth surfaces of the fibers and the debonding at matrix/fiber interface show weak interfacial bonding.In contrast, surfaces of glass fibers in the modified specimen are not smooth (see **Figure 26**(d) and (h)), which is a clear indication of strong adhesion at the interface. Furthermore, it can be observed that the fracture surfaces of the reinforced FML (**Figure 26**(d) and (f)) are remarkably different compared to

those of the reinforced one (**Figure 26**(e)). This change from smooth to rough surface features on the composite fracture surface suggests that the GNPs have induced the deflection of propagating crack fronts, which introduces off-plane loading and generates new fracture surfaces [58].Accordingly,it can be concluded that this process increases the required strain energy to perforate the reinforcedFML.

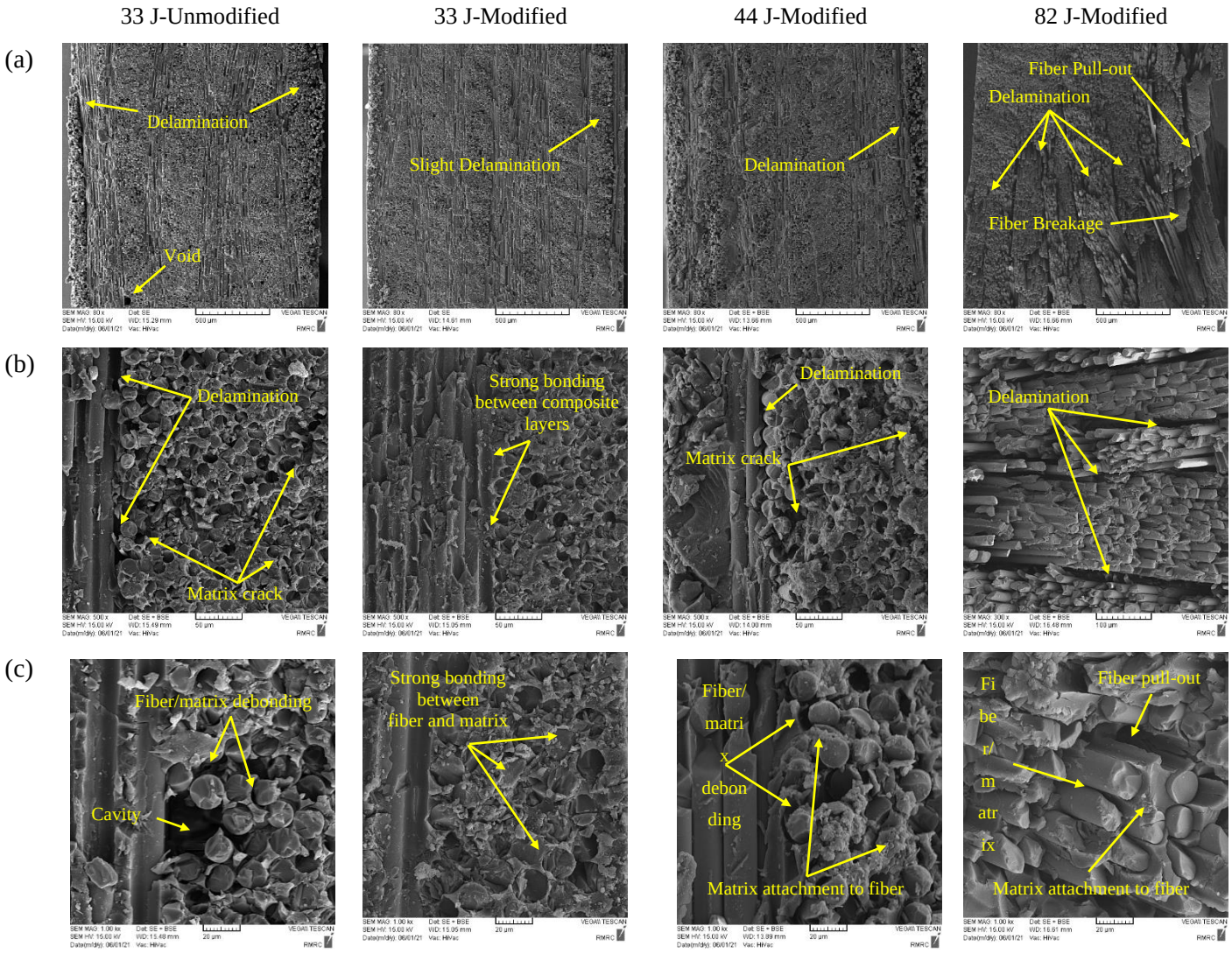

Figure 25. SEM images of FMLsafter impact: (a) over-view of sectional region; (b) and (c) close view of damage mechanism.

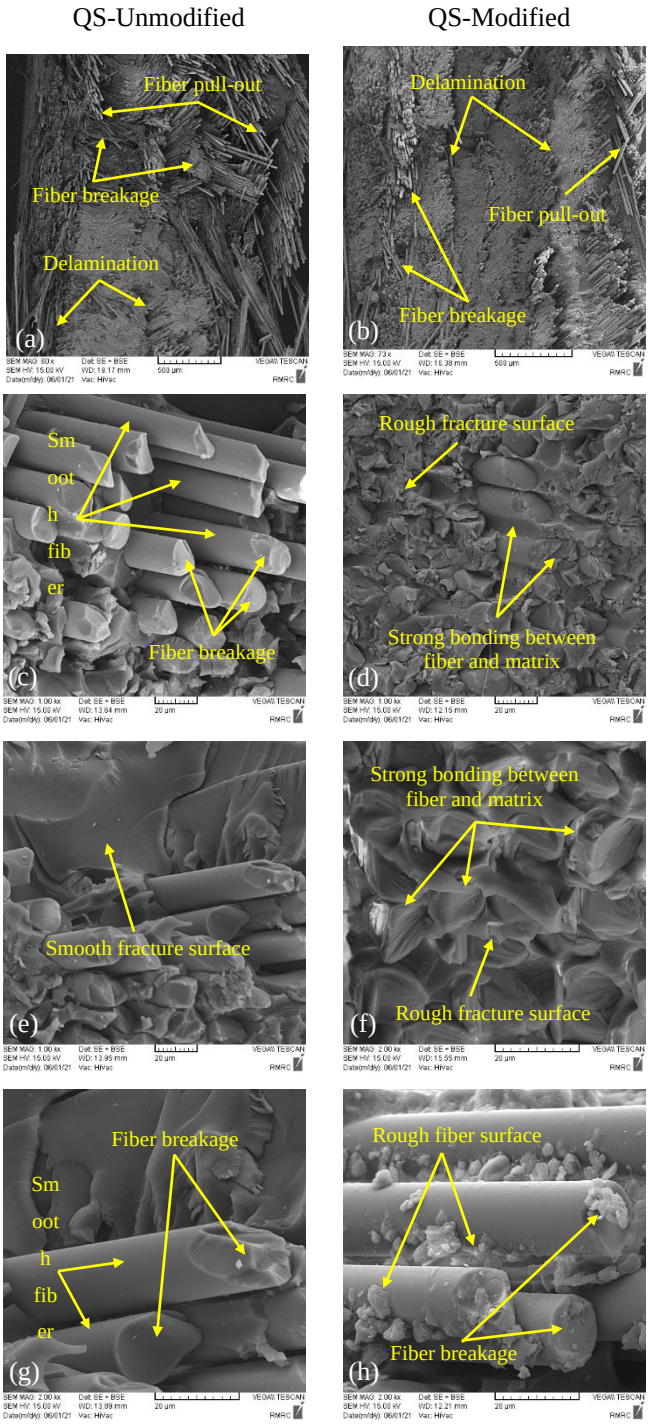

Figure 26. SEM images of FMLs after quasi-static: (a) and (b) over-view of sectional region; (c)-(h) close view of damage mechanism.

As for the SEM images of modified FMLs subjected to different impact energies (**Figure 25**), by increasing impact energy, as expected, delamination, matrix cracking, fiber breakage, fiber pull-out and debonding become more severe. Nevertheless, the matrix attachment to glass fibers is still observed even at 82 J impact energy. Moreover, it is noteworthy that in unreinforced panel under 33 J impact energy, not only the debonding

area and the permanent deformation (**Figure 22**) but also micro damages are more serious than that of reinforced FML at 44 J impact energy, which reveals the remarkable influence of GNPs incorporation.

4 Conclusions

In this work, the influence of incorporation of GNPs on the low-velocity impact behavior of composite and FML specimensis investigated experimentally.The GNPs at a concentration of 0.2 wt% are added to epoxy resin then the reinforced epoxy is used in the fabrication of the composite and FML panels. Impact response and damage pattern ofunmodified and modified panels subjected to various impact energy levels including 33 J, 44J and 82 J are compared. The following conclusions can be drawn from this investigation.

- The inclusion of0.2 wt% of GNPs significantly strengthens the impact resistance of the composite panelso that the modified composite possesses higherbending stiffness,peak load, energy absorption and SEA compared to the unreinforced one.
- For the non-perforated FMLs, the reinforced panelsoffer higher contact stiffness, peak load and SEA and also substantially lower damage area in comparison with the unreinforced ones; for the perforated cases, the behavior of aluminum becomes moredominant so that the inclusion of GNPs has less significant effect on the impact performance of specimens.
- Visual inspections of the damaged area and SEM observations reveal that the addition ofGNPs enhances the adhesion betweenadjacent layers of the composite plies as well as between the resin and fibers, thereby relatively suppressingmatrix/fiber debonding, fiber pull-out, delamination and matrix cracking within the composite laminate of FMLs. Accordingly, it reduces permanent deformation, breakage area and aluminum/composite debonding extent.
- The GNPs incorporation changesthe fracture and fiber surfacesfrom smooth to rough surface features,induces the deflection of propagating crack fronts, and promotes the load transfer capacity from matrix to fibers, thus increasing the impact resistance and the required strain energy to perforate the reinforced FMLs.

- The size of impact damage area, absorbed energy, maximumdeflection and peak load increase with the increasing of impact energy irrespective of the constitution of specimens.
- In aircrafts, low-velocity impact damages often occur on the ground during maintenance operations, service trucks and cargo containers. The results of this study indicate that the incorporation of GNPs has a positive influence on the behavior of specimens when the impact energy is lower than the perforationlimit. Consequently, it is recommended to use GNPs-modified FMLs in the design of new aircraft structures.

Ethical statement

The authors declare that have considered ethical standards, and the paper is compliance with ethical standards.

Funding body

The authors declare that they have no funding body.

Credit author statement

Azadeh Fathi: Conceptualization, Methodology, Investigation, Writing - Original Draft, Writing - Review & Editing. **Gholamhossein Liaghat:** Writing - Review & Editing, Supervision, Project Administration. **Hadi Sabouri:** Investigation, Writing - Review & Editing.

Acknowledgements

The authors declare that they have no acknowledgements.

References

[1] L. Yao, G. Sun, W. He, X. Meng, D. Xie, Investigation on impact behavior of FMLs under multiple impacts with the same total energy: Experimental characterization and numerical simulation, Compos. Struct. 226 (2019) 111218. https://doi.org/10.1016/j.compstruct.2019.111218.

[2] A. Vlot, Fibre Metal Laminates, Springer Netherlands, Dordrecht, 2001. https://doi.org/10.1007/978-94-010-0995-9.

[3] H. Zhang, S.W. Gn, J. An, Y. Xiang, J.L. Yang, Impact Behaviour of GLAREs with MWCNT Modified Epoxy Resins, Exp. Mech. 54 (2014) 83–93. https://doi.org/10.1007/s11340-013-9724-7.

[4] G.B. Chai, P. Manikandan, Low velocity impact response of fibre-metal laminates - A review, Compos. Struct. 107 (2014) 363–381. https://doi.org/10.1016/j.compstruct.2013.08.003.

[5] A. Fathi, G. Liaghat, H. Sabouri, M. Chizari, H. Hadavinia, S. Chitsaz Charandabi, Experimental investigation of quasi-static behavior of composite and fiber metal laminate panels modified by graphene nanoplatelets,. https://doi.org/10.1177/0731684420985275.

[6] G. Yu, L. Wu, L. Ma, J. Xiong, Low velocity impact of carbon fiber aluminum laminates, Compos. Struct. 119 (2015) 757–766. https://doi.org/10.1016/j.compstruct.2014.09.054.

[7] A. Vlot, Low-velocity impact loading: On fibre reinforced aluminium laminates (ARALL and GLARE) and other aircraft sheet materials, Delft University of Technology, Delft, 1993.

[8] A. Vlot, Impact loading on fibre metal laminates, Int. J. Impact Eng. 18 (1996) 291–307. https://doi.org/10.1016/0734-743X(96)89050-6.

[9] A. Vlot, M. Krull, Impact damage resistance of various fibre metal laminates, Le J. Phys. IV. 07 (1997) C3-1045-C3-1050. https://doi.org/10.1051/jp4:19973176.

[10] Y. Liu, B. Liaw, Effects of constituents and lay-up configuration on drop-weight tests of fiber-metal

laminates, Appl. Compos. Mater. 17 (2010) 43–62. https://doi.org/10.1007/s10443-009-9119-1.

[11] G.H. Payeganeh, F. Ashenai Ghasemi, K. Malekzadeh, Dynamic response of fiber–metal laminates (FMLs) subjected to low-velocity impact, Thin-Walled Struct. 48 (2010) 62–70. https://doi.org/10.1016/j.tws.2009.07.005.

[12] A. Seyed Yaghoubi, Y. Liu, B. Liaw, Stacking sequence and geometrical effects on low-velocity impact behaviors of Glare 5 (3/2) fiber–metal laminates, J. Thermoplast. Compos. Mater. 25 (2012) 223–247. https://doi.org/10.1177/0892705711408165.

[13] X. Meng, L. Yao, C. Wang, W. He, L. Xie, H. Zhang, Investigation on the low-velocity impact behaviour of non-symmetric FMLs—experimental and numerical methods, Int. J. Crashworthiness. 0 (2020) 1–19. https://doi.org/10.1080/13588265.2020.1777619.

[14] E.G. Arhore, M. Yasaee, Lay-up optimisation of fibre–metal laminates panels for maximum impact absorption, J. Compos. Mater. 54 (2020) 4591–4609. https://doi.org/10.1177/0021998320937396.

[15] P. Jakubczak, J. Bienias, B. Surowska, The influence of fibre orientation in aluminium–carbon laminates on low-velocity impact resistance, J. Compos. Mater. 52 (2018) 1005–1016. https://doi.org/10.1177/0021998317719569.

[16] I. Şen, R.C. Alderliesten, R. Benedictus, Lay-up optimisation of fibre metal laminates based on fatigue crack propagation and residual strength, Compos. Struct. 124 (2015) 77–87. https://doi.org/10.1016/j.compstruct.2014.12.060.

[17] C.A.J.R.J.R. Vermeeren, An Historic Overview of the Development of Fibre Metal Laminates, Appl. Compos. Mater. 10 (2003) 189–205. https://doi.org/10.1023/A:1025533701806.

[18] M. Sadighi, R.C. Alderliesten, R. Benedictus, Impact resistance of fiber-metal laminates: A review, Int. J. Impact Eng. 49 (2012) 77–90. https://doi.org/10.1016/j.ijimpeng.2012.05.006.

[19] M. Sadighi, T. Pärnänen, R.C. Alderliesten, M. Sayeaftabi, R. Benedictus, Experimental and numerical investigation of metal type and thickness effects on the impact resistance of fiber metal laminates, Appl. Compos. Mater. 19 (2012) 545–559. https://doi.org/10.1007/s10443-011-9235-6.

[20] P. Jakubczak, J. Bieniaś, M. Droździel, The collation of impact behaviour of titanium/carbon, aluminum/carbon and conventional carbon fibres laminates, Thin-Walled Struct. 155 (2020). https://doi.org/10.1016/j.tws.2020.106952.

[21] R. Alderliesten, C. Rans, R. Benedictus, The applicability of magnesium based Fibre Metal Laminates in aerospace structures, Compos. Sci. Technol. 68 (2008) 2983–2993. https://doi.org/10.1016/j.compscitech.2008.06.017.

[22] T. Pärnänen, R. Alderliesten, C. Rans, T. Brander, O. Saarela, Applicability of AZ31B-H24 magnesium in Fibre Metal Laminates - An experimental impact research, Compos. Part A Appl. Sci. Manuf. 43 (2012) 1578–1586. https://doi.org/10.1016/j.compositesa.2012.04.008.

[23] Y. Chen, L. Chen, Q. Huang, Z. Zhang, Effect of metal type on the energy absorption of fiber metal laminates under low-velocity impact, Mech. Adv. Mater. Struct. (2021) in press. https://doi.org/10.1080/15376494.2021.1933659.

[24] A.P. Sharma, S.H. Khan, Influence of metal layer distribution on the projectiles impact response of glass fiber reinforced aluminum laminates, Polym. Test. 70 (2018) 320–347. https://doi.org/10.1016/j.polymertesting.2018.07.005.

[25] A.P. Sharma, S.H. Khan, R. Kitey, V. Parameswaran, Effect of through thickness metal layer distribution on the low velocity impact response of fiber metal laminates, Polym. Test. 65 (2018) 301–312. https://doi.org/10.1016/j.polymertesting.2017.12.001.

[26] J. Bienias, P. Jakubczak, K. Dadej, Low-velocity impact resistance of aluminium glass laminates - Experimental and numerical investigation, Compos. Struct. 152 (2016) 339–348.

https://doi.org/10.1016/j.compstruct.2016.05.056.

[27] P. Jakubczak, J. Bieniaś, M. Droździel, P. Podolak, A. Harmasz, The effect of layer thicknesses in hybrid titanium-carbon laminates on low-velocity impact response, Materials (Basel). 13 (2020). https://doi.org/10.3390/MA13010103.

[28] H. Ahmadi, H. Sabouri, G. Liaghat, E. Bidkhori, Experimental and numerical investigation on the high velocity impact response of GLARE with different thickness ratio, Procedia Eng. 10 (2011) 869–874. https://doi.org/10.1016/j.proeng.2011.04.143.

[29] A. Seyed Yaghoubi, Y. Liu, B. Liaw, Low-Velocity Impact on GLARE 5 Fiber-Metal Laminates: Influences of Specimen Thickness and Impactor Mass, J. Aerosp. Eng. 25 (2012) 409–420. https://doi.org/10.1061/(ASCE)AS.1943-5525.0000134.

[30] P. Compston, W.J. Cantwell, C. Jones, N. Jones, Impact perforation resistance and fracture mechanisms of a thermoplastic based fiber-metal laminate, J. Mater. Sci. Lett. 20 (2001) 597–599. https://doi.org/10.1023/A:1010904930497.

[31] L. Yao, C. Wang, W. He, S. Lu, D. Xie, Influence of impactor shape on low-velocity impact behavior of fiber metal laminates combined numerical and experimental approaches, Thin-Walled Struct. 145 (2019) 106399. https://doi.org/10.1016/j.tws.2019.106399.

[32] L. Ferrante, F. Sarasini, J. Tirillò, L. Lampani, T. Valente, P. Gaudenzi, Low velocity impact response of basalt-aluminium fibre metal laminates, Mater. Des. 98 (2016) 98–107. https://doi.org/10.1016/j.matdes.2016.03.002.

[33] G.C. Jacob, J.M. Starbuck, J.F. Fellers, S. Simunovic, R.G. Boeman, Strain rate effects on the mechanical properties of polymer composite materials, J. Appl. Polym. Sci. 94 (2004) 296–301. https://doi.org/10.1002/app.20901.

[34] F.D. Morinire, R.C. Alderliesten, R. Benedictus, Modelling of impact damage and dynamics in fibre-metal laminates - A review, Int. J. Impact Eng. 67 (2014) 27–38. https://doi.org/10.1016/j.ijimpeng.2014.01.004.

[35] F.D. Morinière, R.C. Alderliesten, M. Sadighi, R. Benedictus, An integrated study on the low-velocity impact response of the GLARE fibre-metal laminate, Compos. Struct. 100 (2013) 89–103. https://doi.org/10.1016/j.compstruct.2012.12.016.

[36] N.A. Nassir, R.S. Birch, W.J. Cantwell, D.R. Sierra, S.P. Edwardson, G. Dearden, Z.W. Guan, Experimental and numerical characterization of titanium-based fibre metal laminates, Compos. Struct. 245 (2020) 112398. https://doi.org/10.1016/j.compstruct.2020.112398.

[37] M. Sadighi, M. Yarmohammad Tooski, R.C. Alderliesten, An experimental study on the low velocity impact resistance of fibre metal laminates under successive impacts with reduced energies, Aerosp. Sci. Technol. 67 (2017) 54–61. https://doi.org/10.1016/j.ast.2017.03.042.

[38] G. Belingardi, M.P. Cavatorta, D. Salvatore Paolino, M.P.C. Ã, D.S. Paolino, Repeated impact response of hand lay-up and vacuum infusion thick glass reinforced laminates, Int. J. Impact Eng. 35 (2008) 609–619. https://doi.org/10.1016/j.ijimpeng.2007.02.005.

[39] G.R. Rajkumar, M. Krishna, H.N. Narasimha Murthy, S.C. Sharma, K.R. Vishnu Mahesh, Experimental Investigation of Low-Velocity Repeated Impacts on Glass Fiber Metal Composites, J. Mater. Eng. Perform. 21 (2012) 1485–1490. https://doi.org/10.1007/s11665-011-0038-6.

[40] O.S. David-West, D.H. Nash, W.M. Banks, An experimental study of damage accumulation in balanced CFRP laminates due to repeated impact, Compos. Struct. 83 (2008) 247–258. https://doi.org/10.1016/j.compstruct.2007.04.015.

[41] J. Bieniaś, P. Jakubczak, B. Surowska, K. Dragan, Low-energy impact behaviour and damage characterization of carbon fibre reinforced polymer and aluminium hybrid laminates, Arch. Civ. Mech.

Eng. 15 (2015) 925–932. https://doi.org/10.1016/j.acme.2014.09.007.

[42] P. Jakubczak, J. Bieniaś, K. Dadej, Experimental and numerical investigation into the impact resistance of aluminium carbon laminates, Compos. Struct. 244 (2020). https://doi.org/10.1016/j.compstruct.2020.112319.

[43] H. Khoramishad, H. Alikhani, S. Dariushi, An experimental study on the effect of adding multi-walled carbon nanotubes on high-velocity impact behavior of fiber metal laminates, Compos. Struct. 201 (2018) 561–569. https://doi.org/10.1016/j.compstruct.2018.06.085.

[44] A.A. Khurram, R. Hussain, H. Afzal, A. Akram, T. Subhanni, Carbon nanotubes for enhanced interface of fiber metal laminate, Int. J. Adhes. Adhes. 86 (2018) 29–34. https://doi.org/10.1016/j.ijadhadh.2018.08.008.

[45] K. Jin, H. Wang, J. Tao, X. Zhang, Interface strengthening mechanisms of Ti/CFRP fiber metal laminate after adding MWCNTs to resin matrix, Compos. Part B Eng. 171 (2019) 254–263. https://doi.org/10.1016/j.compositesb.2019.05.005.

[46] M.A. Abd El-baky, M.A. Attia, Experimental study on the improvement of mechanical properties of GLARE using nanofillers, Polym. Compos. 41 (2020) 4130–4143. https://doi.org/10.1002/pc.25699.

[47] K. Logesh, P. Hariharasakthisudhan, B.S. Rajan, A.A.M. Moshi, V. Khalkar, Effect of multi-walled carbon nano-tube on mechanical behavior of glass laminate aluminum reinforced epoxy composites, Polym. Compos. 41 (2020) 4849–4860. https://doi.org/10.1002/pc.25757.

[48] R. Eslami-Farsani, H. Aghamohammadi, S.M.R. Khalili, H. Ebrahimnezhad-Khaljiri, H. Jalali, Recent trend in developing advanced fiber metal laminates reinforced with nanoparticles: A review study, J. Ind. Text. (2020) 152808372094710. https://doi.org/10.1177/1528083720947106.

[49] L. Li, L. Lang, S. Khan, Y. Wang, Investigation into effect of the graphene oxide addition on the

mechanical properties of the fiber metal laminates, Polym. Test. 91 (2020) 106766. https://doi.org/10.1016/j.polymertesting.2020.106766.

[50] X. Wu, H. Ning, Y. Liu, N. Hu, F. Liu, S. Wang, K. Huang, Y. Jiao, S. Weng, Q. Liu, L. Wu, Synergistic Delamination Toughening of Glass Fiber-Aluminum Laminates by Surface Treatment and Graphene Oxide Interleaf, Nanoscale Res. Lett. 15 (2020). https://doi.org/10.1186/s11671-020-03306-z.

[51] F. Bahari-Sambran, R. Eslami-Farsani, S. Arbab Chirani, The flexural and impact behavior of the laminated aluminum-epoxy/basalt fibers composites containing nanoclay: An experimental investigation, J. Sandw. Struct. Mater. 22 (2020) 1931–1951. https://doi.org/10.1177/1099636218792693.

[52] M. Megahed, M.A. Abd El-baky, A.M. Alsaeedy, A.E. Alshorbagy, An experimental investigation on the effect of incorporation of different nanofillers on the mechanical characterization of fiber metal laminate, Compos. Part B Eng. 176 (2019) 107277. https://doi.org/10.1016/j.compositesb.2019.107277.

[53] M. Rahman, M. Hosur, S. Zainuddin, U. Vaidya, A. Tauhid, A. Kumar, J. Trovillion, S. Jeelani, Effects of amino-functionalized MWCNTs on ballistic impact performance of E-glass/epoxy composites using a spherical projectile, Int. J. Impact Eng. 57 (2013) 108–118. https://doi.org/10.1016/j.ijimpeng.2013.01.011.

[54] X. Zhang, Y. Hu, H. Li, J. Tian, X. Fu, Y. Xu, Y. Lu, Y. Chen, L. Qin, J. Tao, Effect of multi-walled carbon nanotubes addition on the interfacial property of titanium-based fiber metal laminates, Polym. Compos. 39 (2018) E1159–E1168. https://doi.org/10.1002/pc.24670.

[55] D.G. Papageorgiou, I.A. Kinloch, R.J. Young, Mechanical properties of graphene and graphene-based nanocomposites, Prog. Mater. Sci. 90 (2017) 75–127. https://doi.org/10.1016/j.pmatsci.2017.07.004.

[56] Y. Wan, L. Tang, L. Gong, D. Yan, Y. Li, Grafting of epoxy chains onto graphene oxide for epoxy composites with improved mechanical and thermal properties, Carbon N. Y. 69 (2013) 467–480. https://doi.org/10.1016/j.carbon.2013.12.050.

[57] K. Schulte, S. Chandrasekaran, C. Viets, B. Fiedler, New functions in polymer composites using a nanoparticle-modified matrix, in: Multifunct. Polym. Compos. Challenges New Solut., Elsevier Inc., 2015: pp. 875–902. https://doi.org/10.1016/B978-0-323-26434-1.00030-1.

[58] R. Umer, Y. Li, Y.Y. Dong, H.J. Haroosh, K. Liao, The effect of graphene oxide (GO) nanoparticles on the processing of epoxy/glass fiber composites using resin infusion, Int. J. Adv. Manuf. Technol. 81 (2015) 2183–2192. https://doi.org/10.1007/s00170-015-7427-1.

[59] C. Lee, X.D. Wei, J.W. Kysar, J. Hone, D.M. Tartakovsky, S. Broyda, Measurement of the elastic properties and intrinsic strength of monolayer graphene, Science (80-.). 321 (2008) 385–388. https://doi.org/10.1016/j.jconhyd.2010.08.009.

[60] M.A. Rafiee, J. Rafiee, Z. Wang, H. Song, Z. Yu, N. Koratkar, Enhanced mechanical properties of nanocomposites at low graphene content, ACS Nano. 3 (2009) 3884–3890. https://doi.org/10.1021/nn9010472.

[61] A.S. Rahman, V. Mathur, R. Asmatulu, Effect of nanoclay and graphene inclusions on the low-velocity impact resistance of Kevlar-epoxy laminated composites, Compos. Struct. 187 (2018) 481–488. https://doi.org/10.1016/j.compstruct.2017.12.054.

[62] U.A. Shakil, S. Bin Abu Hassan, M.Y. Yahya, Mujiyono, D. Nurhadiyanto, A review of properties and fabrication techniques of fiber reinforced polymer nanocomposites subjected to simulated accidental ballistic impact, Thin-Walled Struct. 158 (2021) 107150. https://doi.org/10.1016/j.tws.2020.107150.

[63] D.W. Lee, J. Il Song, Research on simple joint method using fiber-metal laminate design for improved mechanical properties of CFRP assembly structure, Compos. Part B Eng. 164 (2019) 358–367. https://doi.org/10.1016/j.compositesb.2018.11.081.

[64] M.S. Aswathnarayan, M. Muniraju, H.N. Reddappa, B.M. Rudresh, Synergistic effect of nano graphene on the mechanical behaviour of glass-epoxy polymer composites, Mater. Today Proc. 20 (2020) 177–

184. https://doi.org/10.1016/j.matpr.2019.10.166.

[65] S. Turaka, K. Vijaya Kumar Reddy, Effect of hybrid MWCNTs/graphene on mechanical properties of reinforced unidirectional E-glass/epoxy composite, Mater. Today Proc. 18 (2019) 1540–1547. https://doi.org/10.1016/j.matpr.2019.06.624.

[66] A. Elmarakbi, R. Ciardiello, A. Tridello, F. Innocente, B. Martorana, F. Bertocchi, F. Cristiano, M. Elmarakbi, G. Belingardi, Effect of graphene nanoplatelets on the impact response of a carbon fibre reinforced composite, Mater. Today Commun. 25 (2020) 101530. https://doi.org/10.1016/j.mtcomm.2020.101530.

[67] N. Domun, C. Kaboglu, K.R. Paton, J.P. Dear, J. Liu, B.R.K. Blackman, G. Liaghat, H. Hadavinia, Ballistic impact behaviour of glass fibre reinforced polymer composite with 1D/2D nanomodified epoxy matrices, Compos. Part B Eng. 167 (2019) 497–506. https://doi.org/10.1016/j.compositesb.2019.03.024.

[68] S. Chandrasekaran, C. Seidel, K. Schulte, Preparation and characterization of graphite nano-platelet (GNP)/epoxy nano-composite: Mechanical, electrical and thermal properties, Eur. Polym. J. 49 (2013) 3878–3888. https://doi.org/10.1016/j.eurpolymj.2013.10.008.

[69] S. Rehman, S. Akram, A. Kanellopoulos, A. Elmarakbi, G. Karagiannidis, Thermochimica Acta Development of new graphene / epoxy nanocomposites and study of cure kinetics , thermal and mechanical properties, Thermochim. Acta. 694 (2020) 178785. https://doi.org/10.1016/j.tca.2020.178785.

[70] N. Domun, H. Hadavinia, T. Zhang, G. Liaghat, S. Vahid, C. Spacie, K.R. Paton, T. Sainsbury, Improving the fracture toughness properties of epoxy using graphene nanoplatelets at low filler content, Nanocomposites. 3 (2017) 85–96. https://doi.org/10.1080/20550324.2017.1365414.

[71] Y.C. Chiou, H.Y. Chou, M.Y. Shen, Effects of adding graphene nanoplatelets and nanocarbon aerogels to epoxy resins and their carbon fiber composites, Mater. Des. 178 (2019) 107869.

https://doi.org/10.1016/j.matdes.2019.107869.

[72] M.R. Zakaria, M.H. Abdul Kudus, H. Md. Akil, M.Z. Mohd Thirmizir, Comparative study of graphene nanoparticle and multiwall carbon nanotube filled epoxy nanocomposites based on mechanical, thermal and dielectric properties, Compos. Part B Eng. 119 (2017) 57–66. https://doi.org/10.1016/j.compositesb.2017.03.023.

[73] B. Ahmadi-Moghadam, M. Sharafimasooleh, S. Shadlou, F. Taheri, Effect of functionalization of graphene nanoplatelets on the mechanical response of graphene/epoxy composites, Mater. Des. 66 (2015) 142–149. https://doi.org/10.1016/j.matdes.2014.10.047.

[74] B.A. Selim, Z. Liu, Impact analysis of functionally-graded graphene nanoplatelets-reinforced composite plates laying on Winkler-Pasternak elastic foundations applying a meshless approach, Eng. Struct. 241 (2021) 112453. https://doi.org/10.1016/j.engstruct.2021.112453.

[75] R. Keshavarz, H. Aghamohammadi, R. Eslami-Farsani, The effect of graphene nanoplatelets on the flexural properties of fiber metal laminates under marine environmental conditions, Int. J. Adhes. Adhes. 103 (2020) 102709. https://doi.org/10.1016/j.ijadhadh.2020.102709.

[76] Z. Asaee, M. Mohamed, S. Soumik, F. Taheri, Experimental and numerical characterization of delamination buckling behavior of a new class of GNP-reinforced 3D fiber-metal laminates, Thin-Walled Struct. 112 (2017) 208–216. https://doi.org/10.1016/j.tws.2016.12.015.

[77] S.N. Hosseini Abbandanak, M. Abdollahi Azghan, A. Zamani, M. Fallahnejad, R. Eslami-Farsani, H. Siadati, Effect of graphene on the interfacial and mechanical properties of hybrid glass/Kevlar fiber metal laminates, J. Ind. Text. (2020) 1528083720932222. https://doi.org/10.1177/1528083720932222.

[78] Z. Asaee, M. Mohamed, D. De Cicco, F. Taheri, Low-Velocity Impact Response and Damage Mechanism of 3D Fiber-Metal Laminates Reinforced with Amino-Functionalized Graphene Nanoplatelets, Int. J. Compos. Mater. 7 (2017) 20–36. https://doi.org/10.5923/j.cmaterials.20170701.03.

[79] H. Yaghoobi, F. Mottaghian, F. Taheri, Enhancement of buckling response of stainless steel-based 3D-fiber metal laminates reinforced with graphene nanoplatelets: Experimental and numerical assessments, Thin-Walled Struct. 165 (2021) 107977. https://doi.org/10.1016/j.tws.2021.107977.

[80] ASTM D2651, Standard Guide for Preparation of Metal Surfaces for Adhesive Bonding, 01 (2016) 5–10.

[81] J. Bishopp, Chapter 4 Surface pretreatment for structural bonding, in: Handb. Adhes. Sealants, 2005: pp. 163–214. https://doi.org/10.1016/S1874-5695(02)80005-7.

[82] H. Sabouri, H. Ahmadi, G. Liaghat, Ballistic Impact Perforation into GLARE Targets: Experiment, Numerical Modelling and Investigation of Aluminium Stacking Sequence, Int. J. Veh. Struct. Syst. 3 (2011) 178–183. https://doi.org/10.4273/ijvss.3.3.05.

[83] M. Sangsefidi, H. Sabouri, M. Mir, A. Hasanpour, High-velocity impact response of fiber metal laminates: Experimental investigation of projectile's deformability, Thin-Walled Struct. 159 (2021) 107169. https://doi.org/10.1016/j.tws.2020.107169.

[84] V. Guerra, C. Wan, V. Degirmenci, J. Sloan, D. Presvytis, M. Watson, T. McNally, Characterisation of graphite nanoplatelets (GNP) prepared at scale by high-pressure homogenisation, J. Mater. Chem. C. 7 (2019) 6383–6390. https://doi.org/10.1039/c9tc01361j.

[85] K. Alasvand Zarasvand, H. Golestanian, Investigating the effects of number and distribution of GNP layers on graphene reinforced polymer properties: Physical, numerical and micromechanical methods, Compos. Sci. Technol. 139 (2017) 117–126. https://doi.org/10.1016/j.compscitech.2016.12.024.

[86] P. Jojibabu, Y.X. Zhang, A.N. Rider, J. Wang, R. Wuhrer, B.G. Prusty, High-performance epoxy-based adhesives modified with functionalized graphene nanoplatelets and triblock copolymers, Int. J. Adhes. Adhes. 98 (2020) 102521. https://doi.org/10.1016/j.ijadhadh.2019.102521.

[87] C. Atas, Y. Akgun, O. Dagdelen, B.M. Icten, M. Sarikanat, An experimental investigation on the low

velocity impact response of composite plates repaired by VARIM and hand lay-up processes, Compos. Struct. 93 (2011) 1178–1186. https://doi.org/10.1016/j.compstruct.2010.10.002.

[88] M.R. Abdullah, W.J. Cantwell, The impact resistance of polypropylene-based fibre–metal laminates, Compos. Sci. Technol. 66 (2006) 1682–1693. https://doi.org/10.1016/j.compscitech.2005.11.008.

[89] H. Ahmadi, G. Liaghat, H. Sabouri, E. Bidkhouri, Investigation on the high velocity impact properties of glass-reinforced fiber metal laminates, J. Compos. Mater. 47 (2013) 1605–1615. https://doi.org/10.1177/0021998312449883.

[90] H. Zarei, T. Brugo, J. Belcari, H. Bisadi, G. Minak, A. Zucchelli, Low velocity impact damage assessment of GLARE fiber-metal laminates interleaved by Nylon 6,6 nanofiber mats, Compos. Struct. 167 (2017) 123–131. https://doi.org/10.1016/j.compstruct.2017.01.079.

[91] P. Feraboli, K.T. Kedward, A new composite structure impact performance assessment program, Compos. Sci. Technol. 66 (2006) 1336–1347. https://doi.org/10.1016/j.compscitech.2005.09.009.

[92] Z. Asaee, S. Shadlou, F. Taheri, Low-velocity impact response of fiberglass/magnesium FMLs with a new 3D fiberglass fabric, Compos. Struct. 122 (2015) 155–165. https://doi.org/10.1016/j.compstruct.2014.11.038.

[93] T. Sreekantha Reddy, K. Mogulanna, K. Gopinadha Reddy, P. Rama Subba Reddy, V. Madhu, Effect of thickness on behaviour of E-glass/epoxy composite laminates under low velocity impact, in: Procedia Struct. Integr., Elsevier B.V., 2019: pp. 265–272. https://doi.org/10.1016/j.prostr.2019.05.034.

[94] G. Wu, J.-M. Yang, H.T. Hahn, The impact properties and damage tolerance and of bi-directionally reinforced fiber metal laminates, J. Mater. Sci. 42 (2007) 948–957. https://doi.org/10.1007/s10853-006-0014-y.

[95] S.Y. Park, W.J. Choi, H.S. Choi, H. Kwon, Effects of surface pre-treatment and void content on GLARE

laminate process characteristics, J. Mater. Process. Technol. 210 (2010) 1008–1016. https://doi.org/10.1016/j.jmatprotec.2010.01.017.

[96] H. Aghamohammadi, R. Eslami-Farsani, A. Tcharkhtchi, The effect of multi-walled carbon nanotubes on the mechanical behavior of basalt fibers metal laminates: An experimental study, Int. J. Adhes. Adhes. 98 (2020). https://doi.org/10.1016/j.ijadhadh.2019.102538.

Figure Captions:

Figure 1. The mechanical behavior comparison of epoxy resin with different percentages of GNPs in tensile, compressive and flexural tests: (a) comparison of strength; (b) comparison of modulus [5].

Figure 2. Schematic diagram of modified epoxy preparation.

Figure 3. Lay-up configuration of FML panels.

Figure 4. (a) Fixture installation on the drop-weight apparatus; (b) schematic of fixture

Figure 5. XRD patterns of: (a) GNPs; (b) unmodified and modified epoxy.

Figure 6. Load–deflection curves of composite and FML panels under quasi-static loading [5].

Figure 7. Damage morphologies of FMLs subjected to quasi-static loading: (a) unmodified panel; (b) modified panel [5]. (Magnification of damaged area is denoted by the circle)

Figure 8. Low-velocity impact response of unmodified and modified composite panels impacted at 33 J: (a) absorbed energy; (b) central deflection; (c) contact force; (d) contact stiffness.

Figure 9. Damage morphologies of composites subjected to 33 J impact energy: (a) unmodified panel; (b) modified panel. (Magnification of damaged area is denoted by the circle)

Figure 10. Low-velocity impact response of unmodified and modified FML panels impacted at 33 J: (a) absorbed energy; (b) central deflection; (c) contact force; (d) contact stiffness.

Figure 11. Damage morphologies of FMLs subjected to 33 J impact energy: (a) unmodified panel; (b) modified panel. (Magnification of damaged area is denoted by the circle)

Figure 12. Low-velocity impact response of unmodified and modified FML panels impacted at 44 J: (a) absorbed energy; (b) central deflection; (c) contact force; (d) contact stiffness.

Figure 13. Damage morphologies of FMLs subjected to 44 J impact energy: (a) unmodified panel; (b) modified panel. (Magnification of damaged area is denoted by the circle)

Figure 14. Low velocity impact response of unmodified and modified FML panels impacted at 82 J: (a) absorbed energy; (b) central deflection; (c) contact force; (d) contact stiffness.

Figure 15. Damage morphologies of FMLs subjected to 82 J impact energy: (a) unmodified panel; (b) modified panel.

Figure 16. The comparison of FML responses under different loading rates.

Figure 17. Absorbed energy-time curves of unmodified FMLs under different impact energies.

Figure 18. Maximum deflection in tested specimens under different impact energies.

Figure 19. Maximum impact energies of tested specimens under different impact energies.

Figure 20. Bending stiffness of tested specimens under different impact energies.

Figure 21. COR curves for the tested FMLs under different impact energies.

Figure 22. CR and X-CT results and corresponding cross-sectional view of tested FMLs.

Figure 23. (a) Breakage (b) Debonding and (c) Total damage areas of the FML panels.

Figure 24. SEM images of Modified FML before impact: (a) over-view of sectional region; (b) close view of composite region; (c) and (d) close view of aluminum/composite bonding

Figure 25. SEM images of FMLs after impact: (a) over-view of sectional region; (b) and (c) close view of damage mechanism.

Figure 26. SEM images of FMLs after quasi-static: (a) and (b) over-view of sectional region; (c)-(h) close view of damage mechanism.

Table Captions:

Table 1. Type and mechanical properties of materials.

Table 2. Summary of the quasi-static indentation and the low-velocity impact results.